HELLENIC REPUBLIC

National and Kapodistrian University of Athens

Department of Biology

Athens International Master's Programme in Neurosciences

Hellenic Pasteur Institute

Laboratory of Cellular and Molecular Neurobiology-Stem Cells

# RESEARCH THESIS PROJECT

## ASTROCYTE DYSFUNCTION IN PARKINSON'S DISEASE: INSIGHTS FROM NEURON-ASTROCYTE INTERACTIONS IN A PATIENT-DERIVED MODEL

Sofia Dede

ID Number:7113112100011

2022-2024

Title: Astrocyte Dysfunction in Parkinson's Disease: Insights from Neuron-Astrocyte Interactions in a Patient-Derived Model
Student Name: Sofia Dede

HELLENIC REPUBLIC

National and Kapodistrian University of Athens

Department of Biology

Athens International Master's Programme in Neurosciences

Hellenic Pasteur Institute

Laboratory of Cellular and Molecular Neurobiology-Stem Cells

# RESEARCH THESIS PROJECT

## ASTROCYTE DYSFUNCTION IN PARKINSON'S DISEASE: INSIGHTS FROM NEURON-ASTROCYTE INTERACTIONS IN A PATIENT-DERIVED MODEL

| **Three Member Evaluation Committee** |
|---|
| Florentia Papastefanaki[1,2]<br>[1]Human Embryonic and Induced Pluripotent Stem Cell Unit, Hellenic Pasteur Institute, Athens, Greece<br>[2]Laboratory of Cellular and Molecular Neurobiology-Stem Cells, Hellenic Pasteur Institute, Athens, Greece |
| Era Taoufik[1]<br>[1]Laboratory of Cellular and Molecular Neurobiology-Stem Cells, Hellenic Pasteur Institute, Athens, Greece |
| Yassemi Koutmani[1]<br>[1]Center of Clinical, Experimental Surgery and Translational Research, Biomedical Research Foundation of the Academy of Athens, Athens, Greece |

2022-2024

Title: Astrocyte Dysfunction in Parkinson's Disease: Insights from Neuron-Astrocyte Interactions in a Patient-Derived Model
Student Name: Sofia Dede

Title: Astrocyte Dysfunction in Parkinson's Disease: Insights from Neuron-Astrocyte Interactions in a Patient-Derived Model
Student Name: Sofia Dede

## Contents

Title: Astrocyte Dysfunction in Parkinson's Disease: Insights from Neuron-Astrocyte Interactions in a Patient-Derived Model
Student Name: Sofia Dede

# Astrocyte Dysfunction in Parkinson's Disease: Insights from Neuron-Astrocyte Interactions in a Patient-Derived Model

Author: Sofia Dede[1,2]

1. Department of Biology, National and Kapodistrian University of Athens, Illisia 15784, Athens, Greece
2. Laboratory of Cellular and Molecular Neurobiology-Stem Cells, Hellenic Pasteur Institute, Athens, Greece

Supervisor: Florentia Papastefanaki[1,2]

1. Laboratory of Cellular and Molecular Neurobiology-Stem Cells, Hellenic Pasteur Institute, Athens, Greece
2. Human Embryonic and Induced Pluripotent Stem Cell Unit, Hellenic Pasteur Institute, Athens, Greece; fpapastefanaki@pasteur.gr

## Scientific summary

Synucleinopathies are a group of neurodegenerative disorders characterized by misfolded α-Synuclein (αSyn) aggregates in the central and peripheral nervous systems. In Parkinson's disease (PD), one of the best-researched mutations is G209A in the SNCA gene resulting in the mutant p.A53T-αSyn protein. The pathological effects of the p.A53T-αSyn mutation have been extensively investigated in neurons, yet the consequences on astrocytes and their contribution to PD pathology are understudied. Here we differentiated induced pluripotent stem cells from PD patients carrying the p.A53T-αSyn mutation and from healthy individuals toward ventral midbrain dopaminergic neurons and astrocytes to investigate their reciprocal communication. Our findings reveal that PD astrocytes struggle with the efficient uptake and degradation of neuronal αSyn aggregates due to disrupted lysosomal function, hindering their ability to relieve neuronal cells from accumulated αSyn. Moreover, PD astrocytes showed an enhanced formation of tunneling nanotubes (TNTs), facilitating αSyn transfer. Conversely, healthy astrocytes demonstrated neuroprotective capabilities, reducing protein aggregate load in neurons and promoting neuronal survival through paracrine signaling. Collectively, this study underscores a critical impact of p.A53T-αSyn on astrocytic endo-lysosomal pathway and secretome composition, placing astrocytes as important contributors to PD

neuropathology and potential targets for therapeutic strategies aimed at restoring neuroprotective functions.

## Περίληψη

Οι συνουκλεϊνοπάθειες αποτελούν μια ομάδα νευροεκφυλιστικών διαταραχών που χαρακτηρίζονται από συσσωματώματα λανθασμένα αναδιπλωμένης α-συνουκλεΐνης (αSyn) στο κεντρικό και περιφερικό νευρικό σύστημα. Στη νόσο Πάρκινσον (PD), μία από τις καλύτερα μελετημένες μεταλλάξεις είναι η G209A στο γονίδιο SNCA με αποτέλεσμα τη μεταλλαγμένη πρωτεΐνη p.A53T-αSyn. Οι παθολογικές επιδράσεις της μετάλλαξης p.A53T-αSyn έχουν διερευνηθεί εκτενώς στους νευρώνες, ωστόσο οι συνέπειες στα αστροκύτταρα και η συμβολή τους στη παθολογία της PD δεν έχουν μελετηθεί επαρκώς. Στην παρούσα εργασία διαφοροποιήσαμε επαγόμενα πολυδύναμα βλαστικά κύτταρα από ασθενείς με PD που φέρουν τη μετάλλαξη p.A53T-αSyn και από υγιείς δότες σε ντοπαμινεργικούς νευρώνες και αστροκύτταρα του κοιλιακού μεσεγκεφάλου με σκοπό να διερευνήσουμε την αμοιβαία επικοινωνία τους. Τα ευρήματά μας αποκαλύπτουν ότι τα PD αστροκύτταρα αντιμετωπίζουν δυσκολία με την αποτελεσματική πρόσληψη και αποικοδόμηση των συσσωματωμάτων νευρωνικής αSyn λόγω διαταραγμένης λυσοσωμικής λειτουργίας, παρεμποδίζοντας την ικανότητά τους να ανακουφίζουν τα νευρωνικά κύτταρα από τη συσσωρευμένη αSyn. Επιπλέον, τα PD αστροκύτταρα παρουσίασαν ενισχυμένο σχηματισμό σηραγγωδών νανοσωληνίσκων (TNTs), διευκολύνοντας τη μεταφορά της αSyn. Αντίθετα, τα υγιή αστροκύτταρα επέδειξαν νευροπροστατευτικές ικανότητες, μειώνοντας το φορτίο των πρωτεϊνικών συσσωματωμάτων στους νευρώνες και προάγοντας τη νευρωνική επιβίωση με παρακρινή σηματοδότηση. Συνολικά, η παρούσα μελέτη υπογραμμίζει τον κρίσιμο αντίκτυπο της p.A53T-αSyn στην αστροκυτταρική ενδο-λυσοσωμική οδό και στη σύσταση του εκκρινώματος, καθιστώντας τα αστροκύτταρα σημαντικούς συντελεστές στη νευροπαθολογία της PD και πιθανούς στόχους για θεραπευτικές προσεγγίσεις που αποσκοπούν στην αποκατάσταση των νευροπροστατευτικών λειτουργιών τους.

## Highlights

- p.A53T-αSyn astrocytes are unable to efficiently uptake and degrade neuronal αSyn aggregates due to lysosomal malfunction.
- p.A53T-αSyn astrocytes are ineffective at clearing αSyn buildup in neurons.
- p.A53T-αSyn astrocytes show enhanced formation of TNTs, likely facilitating αSyn transfer.
- p.A53T-αSyn astrocytes exert a paracrine neurotoxic effect, while healthy astrocytes display non-contact-mediated neuroprotective properties.

## Keywords

induced pluripotent stem cells; lysosomes; alpha-synuclein; tunnelling nanotubes; secretome

## Λέξεις-κλειδιά

επαγόμενα πολυδύναμα βλαστικά κύτταρα; λυσοσώματα; άλφα-συνουκλεΐνη; σηραγγώδεις νανοσωληνίσκοι; εκκρίνωμα

## Lay summary

Parkinson's disease (PD) is a common brain disorder, affecting about 1 in every 100 people over 60. People with PD often have movement problems including tremor, stiffness, and balance issues, along with non-motor symptoms like loss of smell, sleep and memory issues. The disease happens because of a gradual loss of a particular group of neurons (brain cells) that control movement, but we still do not fully understand why, which makes finding a cure difficult. Astrocytes are a different cell population in the brain that keeps neurons healthy, but they have not been adequately examined in PD. In our research, we used skin cells from both PD patients and healthy people to create patient-specific brain cells, astrocytes and neurons, and study how they interact. We found that unlike healthy astrocytes, PD astrocytes struggled to clear out toxic proteins, and could not protect neurons. The PD astrocytes had issues in their intracellular structures responsible for breaking down waste. Additionally, PD astrocytes released harmful molecules instead of protective ones. Our study suggests that the failure of PD astrocytes to remove toxic molecules

and protect neurons may play a key role in PD and could lead to new treatment strategies in the future.

## Introduction

Parkinson's disease (PD) is the second most common neurodegenerative disorder after Alzheimer's disease, affecting approximately 1% of individuals aged > 60 years. The two major histopathological hallmarks of PD are the progressive death of striatal-projecting dopaminergic neurons in the substantia nigra and the presence of intracellular protein inclusions in neuronal perikarya called Lewy Bodies (LB) and neurites (Lewy neurites, LN) (Braak et al., 1999). The clinical manifestations of PD include motor symptoms, such as tremor, rigidity, postural instability, and akinesia/bradykinesia (Bloem et al., 2021). Nevertheless, it is now recognized that the disease involves more widespread neuronal dysfunction, leading to early and late non-motor symptoms including hallucinations, depression, hyposmia, sleep disorders, cognitive decline, and dementia (Schapira & Tolosa, 2010). Although it is still unknown whether dopamine neuron degeneration is an initial disease feature or the inevitable consequence of multiple dysfunctions throughout the brain, it represents a common pathological manifestation in PD and is responsible for many clinical symptoms. PD is currently incurable highlighting the incomplete understanding of the underlying mechanisms.

Most PD cases are sporadic; however, 5-10% of cases have been linked to mutations in specific genes (Deng et al., 2018), such as the SNCA gene encoding α-synuclein (αSyn), the major component of LBs and LNs in its aggregated form, which is also considered to play a central role in their formation (Spillantini et al., 1997). αSyn is a small neuronal protein widely distributed in the CNS with preferential localization at the presynaptic terminals. Its direct association with the synaptic vesicles suggests possible roles in the regulation of neurotransmitter release, synaptic function, and plasticity (Lashuel et al., 2013a). Although the physiological function of αSyn (Bendor et al., 2013) is still under investigation, its involvement in neurodegenerative processes has been clearly defined owing to the identification of multiple disease-causing mutations (Puschmann, 2017; Wong & Krainc, 2017). The best-studied αSyn mutation is p.A53T (G209A in the SNCA gene) which leads to early onset and severe PD pathology (Polymeropoulos et al., 1997). Forced expression of mutant p.A53T-αSyn has led to the development of numerous *in vitro* and *in vivo* animal models that

have been valuable for gaining insights into PD etiopathology (Breger & Fuzzati Armentero, 2019; Lázaro et al., 2017). However, an important limitation is the extent to which these experimental systems recapitulate the key neuropathological features of human diseases.

Unlike the well-studied role of neurons in PD, little is known about the contribution of glial cells, which has recently begun to be appreciated (Zuchero & Barres, 2015). In particular, astrocytes comprise the most abundant glial cell population surrounding neurons in the human brain. Although astrocytes have been traditionally considered passive supporters of neuronal survival, they participate in neuronal development, neural circuit function, and synaptic transmission. Additionally, they constitute central players in the formation of the blood brain barrier (BBB), ion homeostasis, and the glymphatic system, while critically contributing to protein clearance through the endo-lysosomal pathway (Booth et al., 2017; Brandebura et al., 2023; Sloan & Barres, 2014). Moreover, accumulating evidence indicates that astrocytic defects play a central role in the pathology of the central nervous system and could underlie neuronal cell loss in acute or chronic neurodegenerative diseases, either due to loss of capacity to support neuronal health or due to the development of a neurotoxic phenotype, thus contributing to non-cell-autonomous neurodegeneration (di Domenico et al., 2019). Astroglial cells play important roles in modulating synaptic architecture and activity under physiological conditions (De Luca et al., 2018; Miller, 2018), and they adopt a neurotoxic phenotype upon brain injury or disease (Liddelow & Barres, 2017). Additionally, astrocytes may affect neuronal health status and neuronal αSyn-load through secreted mediators without cell-to-cell contact (Barbar, Jain, et al., 2020; di Domenico et al., 2019; Pons-Espinal et al., 2024; Qiao et al., 2016; Sharma et al., 2023; Yang et al., 2022). It is therefore critical to address whether and how the p.A53T-αSyn mutation affects the dynamic interactions among astrocytes and neurons in a non-cell autonomous context in PD.

To date, there is little evidence regarding the expression levels and the physiological role of αSyn in astrocytes. In previous studies, intracellular deposits of aggregated αSyn have been detected within astrocytes (Sorrentino et al., 2019). Astrocytic αSyn-immunoreactive inclusions were reported in sporadic PD autopsies, exhibiting

cortical distribution (Braak et al., 2007), but also in the nigra (Wakabayashi et al., 2000) and other brain regions, displaying a unique signature of post-translational modifications (Altay et al., 2022) that is morphologically distinct from neuronal Lewy pathology (Sorrentino et al., 2019). In line, induced pluripotent stem cell (iPSC)-derived astrocytes from PD patients, express more αSyn compared to astrocytes derived from healthy donors (di Domenico et al., 2019). Alpha-Synuclein can be released as free molecule by neurons upon degeneration and membrane rupture or alternatively it can be secreted enclosed within extracellular vesicles (EVs) (Emmanouilidou et al., 2010a). Transfer of αSyn-containing exosomes from neurons to astrocytes has been reported (Meng et al., 2020). Overall, astrocytic αSyn may originate from endogenous expression, uptake of neuronal αSyn, or both.

An alternative contact-mediated mechanism may underlie αSyn transfer among neurons and astrocytes. Tunneling nanotubes (TNTs), first described by (Rustom et al., 2004), have gained growing interest as an innovative mode of intercellular communication, pivotal for the transport of materials and information among cells. TNTs are defined as straight, dynamic, membrane-continuous channels spiraling at the top of the bottom layer in 2D cell culture, connecting two homotypic or heterotypic cells, allowing the transport of cellular cargo due to their open nature. Their diameter varies between 50 and 700 nm (with an average of 200 nm) and their length may be from tens up to several hundred microns (average 20-100 µm) (Zurzolo, 2021). These cellular extensions allow the transfer of many types of cargoes, from small molecules (e.g., calcium ions) and macromolecules (nucleic acids, proteins, etc.) to entire organelles (lysosomes, mitochondria etc.) between connected cells (Abounit & Zurzolo, 2012). Moreover, TNTs are involved in the cell-to-cell spreading of protein aggregates associated with neurodegenerative diseases, including αSyn and Tau aggregates, aiding the progression of neurodegeneration (Victoria & Zurzolo, 2017). Alpha-Synuclein can be efficiently transferred via TNTs from neurons to astrocytes and from astrocytes to astrocytes, whereas transfer from astrocytes to neurons was less efficient (Loria et al., 2017b). Further, stress-activated astrocytes obtain healthy mitochondria from neighboring healthy astrocytes via TNTs, facilitating cellular energy support (Loria et al., 2017; Rostami et al., 2017a).

Alpha-Synuclein fibrils are mainly localized inside lysosomes in both primary neurons and astrocytes and may be transferred inside lysosomes through TNTs from fibril-loaded donor cells to naive acceptor cells, where αSyn-fibrils are able to induce the aggregation of soluble αSyn (Abounit et al., 2016). Therefore, the contribution of TNTs to spreading of PD neuropathology is highlighted and they could possibly be a prominent pharmacological target. However, the role of TNTs in neuron-astrocyte communication remains understudied and further studies are necessary to unravel their full contribution to PD pathology.

Under normal conditions, astrocytes degrade intracellular aggregates of αSyn, while their translocation from astrocytes to neurons is limited. This suggests that astrocytes play a major role in the degradation rather than in the spreading of αSyn aggregates (Loria et al., 2017). Alpha-Synuclein oligomers or fibrils transferred to astrocytes, colocalize with lysosomal-associated membrane protein (LAMP) 1, indicating its subsequent delivery to lysosomal compartments for degradation (Lindström et al., 2017a; Loria et al., 2017). In line, a study using iPSC-derived dopaminergic neurons and astrocytes showed that the astrocytes rapidly internalized αSyn and exhibited increased lysosomal degradation rates, when compared to neurons. At the same study, co-culture of neurons and astrocytes results in decreased accumulation of αSyn in neurons and αSyn transfer between neurons, suggesting that astrocytes may be neuroprotective by relieving intraneuronal accumulation of αSyn and clearing excessive extracellular αSyn load (Tsunemi et al., 2020). In familial PD, astrocytes carrying mutations in *LRRK2 (PARK8)*, *GBA1*, and *ATP13A2 (PARK9)* exhibited reduced degradation capacity to various extents and aggravated αSyn accumulation, promoting neurodegeneration (Aflaki et al., 2020; di Domenico et al., 2019; Henry et al., 2015; Tsunemi et al., 2020). Therefore, preservation of normal lysosomal function in astrocytes is of high essence to support neuronal health and loss of this function may lead to propagation of PD pathology.

Unpublished data from our lab demonstrate that iPSC-derived astrocytes from PD patients with the p.A53T-αSyn mutation display cell-autonomous pathological phenotypes, toxic αSyn accumulation, and inability to support neuronal fitness. In

the absence of neurons, a significant increase in p(Ser129)αSyn expression, as well as in the number and size of p(Ser129)αSyn$^{+}$ puncta, and cytoplasmic protein aggregates, were noted in p.A53T-αSyn astrocytes, compared to healthy astrocytes. Additionally, impaired phagocytic activity was detected in p.A53T-αSyn astrocytes when exposed to pHRodo-*E. coli* bioparticles. Proteomic analysis revealed failure of major proteostasis mechanisms in PD iAstrocytes, largely related to lysosomal malfunction. Lastly, in a neuron-astrocyte co-culture setup p.A53T-αSyn astrocytes induced PD-relevant neuropathology to healthy neurons, while healthy astrocytes alleviated neuropathology in co-culture with PD neurons (Paschou, Apokotou et al., under submission).

Despite intensive research, no effective PD treatment has been established. Given the multiple roles attributed to glial cells both in physiology and disease of the nervous system, the fundamental hypothesis of this study is that the understudied contribution of neuron-glia interactions in the underlying mechanisms of PD contains unidentified components that could prove useful in the design of effective therapeutic approaches. Therefore, the objective of this study was to thoroughly understand the glia-related non-cell-autonomous compartment of PD pathology, also taking into consideration the transmissible nature of PD that has been suggested to manifest through cell-to-cell transfer of αSyn aggregates (Lashuel et al., 2013b; Rostami et al., 2020). We differentiated iPSC lines obtained from PD patients carrying the p.A53T-αSyn mutation and controls toward ventral midbrain (vm) dopaminergic neurons and astrocytes to investigate their reciprocal communication. The specific aims of this study were to examine whether PD astrocytes abolish critical functions related with the transfer, uptake, and degradation of αSyn aggregates, thus affecting neuronal health status. Additionally, we asked whether astrocytes influence neuronal pathophysiology through secretion of paracrine mediators without cell-to-cell contact.

## Methods

### Ethics Statement

This study involves existing induced pluripotent stem cell (iPSC) lines (Kouroupi et al., 2017; Soldner et al., 2011) derived in accordance with established ethical guidelines

and distributed under Material Transfer Agreements to ensure compliance with all legal and ethical standards.

### Culture of human induced pluripotent stem cells (iPSCs)

The iPSCs used included lines from two male PD patients (PD1 and PD2) carrying the G209A (p.A53T) SNCA mutation and one age- and sex-matched non-PD healthy subject (H1) (two different clones from each subject), previously generated in our lab (Kouroupi et al., 2017); an age- and sex-matched non-PD healthy line (H2) obtained from the New York Stem Cell Foundation; a female PD iPSC line (PD3) carrying the G209A SNCA mutation and its gene-corrected isogenic control line ($PD3^{corr}$)(Soldner et al., 2011) (Table 1). iPSCs were cultured either on mouse embryonic fibroblasts (Thermo Fisher Scientific) or under feeder-free conditions on Matrigel (BD Biosciences), following standard procedures. iPSCs were quality checked according to the ISSCR standards (Ludwig et al., 2023) for karyotype integrity, mycoplasma contamination, undifferentiated state and pluripotency, and presence of the disease mutation.

### Differentiation of iPSCs into midbrain-patterned Neural Precursor cells

To generate midbrain-patterned neural precursor cells (NPC) we used previously published methods (de Rus Jacquet, 2019; Kriks et al., 2011) on iPSCs dissociated to single cells with accutase (Thermo Fisher Scientific). On day 11, the cells were replated at 700,000 cells/$cm^2$ on Geltrex and the culture medium was switched to NPC medium [Neurobasal, 2%, B27 supplement (minus vitamin A), (Thermo Fisher Scientific); 20 ng/ml fibroblast growth factor-2 (FGF-2; Peprotech), and 20 ng/ml epidermal growth factor (EGF; Peprotech)] supplemented with 3 µM CHIR99021 (Stemgent). From day 13, the cells were maintained in NPC medium. All reagents used in cell cultures are listed in Table 2. Upon passages 1 or 2, NPCs were quality checked for regional identity. Only those NPCs that passed the quality control were used for differentiations.

### Differentiation of Neural Precursor cells into Dopaminergic Neurons

To prepare dopaminergic neurons, NPCs were harvested using accutase (Thermo Fisher Scientific) and plated at 6,000,000 cells/well on a Geltrex-coated 6-well plate. When NPCs reached at least 80% confluency, the medium was switched to neuronal

differentiation medium [Neurobasal, 2% (v/v) B27 supplement plus, 1% (v/v) N2 supplement, 1% (v/v) GlutaMAX, 100 U/ml penicillin-streptomycin] supplemented with 0.5 mM dibutyryl cyclic AMP (dbcAMP, Sigma Aldrich), 10 µM γ-secretase inhibitor (DAPT, Tocris), 0.2 mM ascorbic acid (Sigma Aldrich), 20 ng/ml brain-derived growth factor (BDNF; Peprotech), 20 ng/ml glial-derived growth factor (GDNF; Peprotech), 1 ng/ml transforming growth factor-β3 (TGF-β3; Peprotech) (de Rus Jacquet, 2019; Kriks et al., 2011). Neuronal differentiation medium was replenished every 2 days for a total of 21 days. Following differentiation, neurons were dissociated with accutase and plated on PLO/Laminin-coated plates (250,000 - 300.000 cells/cm$^2$) for conditioned media experiments. In the rest of the text iPSC-derived neurons will be referred as iNeurons.

### Differentiation of Neural Precursor cells into Astrocytes

For astrocytic differentiation, we adopted established protocols (de Rus Jacquet, 2019). To initiate differentiation, midbrain-patterned NPCs (after at least 4 weeks of expansion in NPC medium) were plated at 15,000 cells/cm$^2$, continuously maintained in astrocyte differentiation medium (AM, Sciencell), and passaged approximately every 7 days, until day 28. The plating density and the passaging schedule were adjusted depending on the line. Both NPCs and iPSC-derived astrocytes were cryopreserved in 90% Fetal Bovine Serum (FBS) and 10% dimethyl sulfoxide (DMSO) at intermediate passages. In the rest of the text iPSC-derived astrocytes will be referred as iAstrocytes.

### Maturation of iAstrocytes

iAstrocytes were plated at 30,000 cells/cm$^2$ on Geltrex and on day 0, AM was switched to Astro-Maturation Medium [Advanced DMEM/F-12, 2% B27 (minus vitamin A), 1% Glutamax, 1% N2, 1% non-essential amino-acids, BMP4, and CNTF both 20 ng/µL; Peprotech], for at least 2 weeks. For the first 7 days of maturation the cells were treated with 0.5% FBS, and then FBS was fully withdrawn.

### Astrocyte-Conditioned Medium treatment of iNeurons

The protocol we used for conditioned medium collection was based on previous publications (Barbar, Rusielewicz, et al., 2020; S.-I. Lee et al., 2021), with appropriate adjustments. After the 2-week maturation period, the culture medium of iAstrocytes

(40,000 cells/cm$^2$) was switched to Neuron Basal medium [Neurobasal, 2% (v/v) B27 supplement plus, 1% (v/v) N2 supplement, 1% (v/v) GlutaMAX, 100 U/ml penicillin-streptomycin]. In parallel, iNeurons on differentiation day 21 were replated at 250,000 cells/well on poly-L-ornithine (PLO; 20 µg/ml; Sigma)/ laminin (5 µg/ml; Sigma) -coated glass coverslips in 48-well plates and cultured in Neuronal Differentiation Medium. After 72 h the Astrocyte-Conditioned Medium (ACM) was collected from iAstrocytes and centrifuged (3 min, 500 × g) to spin down any cells and debris that might have detached from the astrocyte plate. Subsequently, the ACM was added to iNeurons. Fresh ACM was transferred to iNeurons every 3 days for 6-7 days. As a control, neurons were cultured in 1:1 Neuron Basal medium /Neuronal Differentiation Medium.

### Neuron-Conditioned Medium treatment of iAstrocytes

Differentiation day-21 PD iNeurons were plated at 300,000 cells/cm$^2$ and cultured in Neuronal Differentiation Medium. Twenty-four h later, iNeurons were switched to Neuron Basal medium. After 48 h, the conditioned medium was collected from PD iNeurons (PDnCM), centrifuged (3 min, 500 × g) and added to mature iAstrocytes plated at 30,000 cells/cm$^2$ for immunofluorescence. iAstrocytes were cultured in PDnCM or Neuron Basal medium (control) for 6 h.

### Treatment of iAstrocytes with αSyn pre-formed fibrils (PFFs)

Human αSyn pre-formed fibrils (PFFs) conjugated with AlexaFluor568 were prepared as described previously (Dilsizoglu Senol et al., 2021; Nonaka et al., 2010). Differentiation day-38 iAstrocytes were plated at 20,000 cells/cm$^2$ on Geltrex in AM. Forty-eight h later, αSyn-PFFs were diluted in AM (500 nM), sonicated, and either added to the astrocytes, for 1, 2, 4, 6, and 16 h of incubation, or added and washed after 2 h, while iAstrocytes remained in culture for 16 h. Cells were imaged fixed under a confocal spinning-disk microscope (Nikon Eclipse Ti2). The number of internalized αSyn-PFFs was recorded per cell, considering the area of each cell as ROI, using Analyze Particles with Auto Threshold after denoising in FIJI (NIH).

### Lysosensor assay

To assess lysosomal acidity, differentiation day-38 iAstrocytes were plated at 150,000 cells/dish on Geltrex-coated 35-mm Ibidi µ-dish, AM. Forty-eight h later, the

fluorescent pH indicator LysoSensor™ Green (1 µM, Thermo Fisher Scientific) was added to iAstrocyte culture medium for 30 min, at 37°C. Subsequently, cells were washed with fresh medium and imaged live under a confocal spinning-disk microscope (Nikon Eclipse Ti2) under environmental conditions at 37°C. All images were acquired with identical settings for laser power from three biological replicates for healthy and PD, including the isogenic pair. The integrated density of LysoSensor green fluorescence was measured per cell with stable manual threshold, considering the area of each cell as region of interest (ROI), in FIJI (NIH).

### Lysotracker staining

For the assessment of lysosomal number and acidity, we used LysoTracker™ Deep Red (50 nM, Thermo Fisher Scientific). Differentiation day-38 iAstrocytes were plated at 150,000 cells/dish on Geltrex-coated 35 mm Ibidi µ-dish in AM. After 48 h, we added LysoTracker to Astrocyte culture medium for 30 min at 37°C. Subsequently, cells were washed with fresh medium and imaged live under a confocal spinning-disk microscope (Nikon Eclipse Ti2) at 37°C. All images were acquired with identical settings for laser power from three biological replicates for healthy and PD, including the isogenic pair. The number of labeled lysosomes was quantified per cell, considering the area of each cell as ROI, using Analyze Particles with stable manual threshold after denoising in FIJI (NIH). Lysosomal acidity was measured as integrated density per cell using constant threshold settings.

### Cathepsin B activity assay

To detect lysosomal Cathepsin B enzymatic activity we utilized the Magic Red® Fluorescent Cathepsin B assay kit (ImmunoChemistry Technologies). Differentiation day-38 iAstrocytes were plated at 150,000 cells/dish on Geltrex-coated 35mm Ibidi µ-dish in AM. After 48 h, iAstrocytes were treated with Magic Red according to manufacturer's instructions for 15 min at 37°C. Cells were then immediately live imaged by confocal spinning-disk microscope (Nikon Eclipse Ti2) at 37°C, within 20 min. The activity of Cathepsin B was detected as red fluorescent vesicles produced by the hydrolysis of the fluorogenic substrate. All images were acquired with identical settings for laser power from three biological replicates for healthy and PD, including the isogenic pair. For quantification, integrated density of red fluorescence was

measured per cell with stable manual threshold, considering the area of each cell as ROI, in FIJI (NIH).

### iAstrocyte-SH-SY5Y co-culture (SH-SY5Y loaded with PFFs)

For neuron-to-astrocyte transfer of αSyn-PFFs, human neuroblastoma GFP$^+$ SH-SY5Y cells were plated at 400,000 cells/well on uncoated 6-well plates in RPMI1640 (Euroclone). Twenty-four h later, human αSyn pre-formed fibrils (PFFs) conjugated with Alexa 568 were added in culture medium for 16 h. PFF-loaded SH-SY5Y cells (donor cells) were then trypsinized, mixed with either healthy or PD iAstrocytes (acceptor cells) at a ratio 1:1, and sub-confluently seeded (~70%) on Geltrex-coated coverslips in 24-well plates in AM. A two-step fixation protocol followed after 24 h of co-culture, as described previously (Chakraborty et al., 2023). Subsequently, cells were stained for F-Actin with Phalloidin 647 (1:300 diluted in 1X PBS, Invitrogen), for 30 min, at 22-23 ℃, in the dark. All images were acquired with identical settings for laser power from three biological replicates for healthy and PD, including the isogenic pair under a confocal spinning-disk microscope (Nikon Eclipse Ti2). The numbers of intracellular αSyn-PFFs in SH-SY5Y cells and iAstrocytes were counted per cell, considering the area of each cell as ROI and using Analyze Particles with Auto Threshold after denoising in FIJI (NIH).

### Labelling Tunneling Nanotubes (TNTs)

Differentiation day-38 iAstrocytes were plated at 35,000 cells/well in Geltrex-coated glass coverslips in 24-well plates and cultured in AM. After cells reached sub-confluency (~70%), a two-step fixation protocol was used to preserve TNTs, as described previously (Chakraborty et al., 2023) and subsequently the plasma membrane of the cells was stained with wheat germ agglutinin (WGA) 647, (1:300 diluted in 1X PBS, Life Technologies), and F-Actin was labeled with Phalloidin 488 (1:300 diluted in 1X PBS, Thermo Fisher Scientific), for 30 min, at 22-23℃, in the dark. All images were acquired under a confocal spinning-disk microscope (Nikon Eclipse Ti2). The number of TNT-connected cells and TNT-connections per cell were determined using the ICY software (https://icy.bioimageanalysis.org/).

### Protein aggregate detection

The presence of protein aggregates in neuronal cultures was examined using the PROTEOSTAT Aggresome Detection Kit (Enzo Life Sciences, ENZ-51035-0025) according to manufacturer's instructions.

### Immunofluorescence

To analyze cultured cells by immunofluorescence, they were plated on glass coverslips and fixed with 4% paraformaldehyde (Sigma- Aldrich) in PBS for 15 min at 22-23 °C. Non-specific binding sites were blocked for 30 min with 5% Normal Donkey Serum (NDS) in PBS, also containing 0.3% Triton X-100 (Sigma-Aldrich) for permeabilization (for intracellular epitopes) and were subsequently incubated with primary antibodies at 4 °C for 16 h, followed by 3 washes with PBS and incubation with the appropriate combination of secondary antibodies (Molecular Probes, ThermoFisher Scientific) conjugated with Alexa Fluor 488, 546, or 647 for at least 1 h at 22-23 °C. The coverslips, after 3 washes with PBS and one with $ddH_2O$, were mounted with StayBrite Hardset Mounting Medium with DAPI (BIOTIUM, 23004) and were let dry for 16 h, at 22-23 °C in the dark before proceeding with confocal imaging. All primary antibodies and their blockings are listed in Table 3. Images were acquired using a Leica TCS SP5II or Leica TCS SP8P confocal microscope (LEICA Microsystems) or confocal spinning-disk microscope (Nikon Eclipse Ti2) and analyzed using the open-source software FIJI (NIH) (Schindelin et al., 2012).

### RNA isolation, cDNA Synthesis and RT-qPCR

Total RNA was extracted from cultured cells using the TRIzol Reagent (Life Technologies, 15596018), according to the manufacturer's guidelines. After measurement of the RNA yield and estimation of the RNA/protein ratio using the Nanodrop spectrophotometer (ThermoFisher Scientific), the samples were processed with RQ1 DNAse (Promega Corporation, M6101) for the digestion of contaminating DNA. RNA samples were further cleaned-up and concentrated using the RNA Clean and Concentrator kit (Zymo Research, R1017). One microgram of total RNA was used for first strand cDNA synthesis using ProtoScript II Reverse Transcriptase (New England BioLabs, M0368) according to the manufacturer's instructions and diluted 1:5 in ddH2O. Quantitative PCR analyses were carried out in a StepOnePlus™ Real-Time PCR detection system (Applied Biosystems) using the SYBR™ Select Master Mix

(Applied Biosystems, 4472908). Transcript expression was determined in triplicate reactions, unless otherwise stated, and normalized to glyceraldehyde-3-phosphate dehydrogenase (GADPH) as housekeeping gene.

### Image analysis and statistics

All measurements, except from TNT-counting, were performed in the open-source software FIJI (NIH) (Schindelin et al., 2012). All experiments were performed in at least 3 biological replicates of healthy and PD samples. Biological replicate is defined at the level of different iPSC clones. For RT-qPCR, each measurement was performed in technical triplicates. In NPC quality control, relative mRNA levels were calculated for each gene by using the 1/ΔCT method with *GADPH* as reference. SNCA mRNA levels were calculated by the $2^{-\Delta\Delta CT}$ method, with the same gene of reference (Livak & Schmittgen, 2001). $CD44^+$, $VIMENTIN^+$, $ALDH1L1^+$, and $S100\beta^+$ iAstrocytes were counted manually and the percentage was calculated relative to total cells (DAPI). The number of p(Ser129)$\alpha Syn^+$ puncta were counted using the "Analyze Particles" plugin, keeping constant threshold settings, considering each cell area as region of interest (ROI). In the assessment of neuronal survival, we calculated manually the total number of $MAP2^+$cells and the percentage of $TH^+$ cells over total $MAP2^+$cells. For network density, we measure the thresholded $MAP2^+$ area over total $MAP2^+$ cells. The neuronal αSyn-load was analyzed by measuring the mean intensity of αSyn in randomly selected $MAP2^+$cells, considering the area of each cell body as ROI. The numbers of $aggresome^+$ cells and double positive for aggresome and conformation specific αSyn cells were counted manually and normalized to the total number of $MAP2^+$ cells. The percentage of TNT-connected cells was analyzed using the ICY software. Images were assessed for TNT connections along the optical slices, and cells were marked to be connected if there existed one or more TNT(s) in the middle stacks connecting two cells. The number of connected cells were counted and normalized to the total number of cells to represent the proportion of TNT-connected cells. The number of TNT-connections per cell was calculated as the average number of TNT-connections formed by each cell. Comparisons between two independent groups were performed using unpaired t-test (for normally distributed sample values) or non-parametric Mann-Whitney analysis (for not normally

distributed sample values) to determine the significance of differences between the two groups. In experimental setups with two independent variables, two-way ANOVA with Sidak post-hoc analysis or Tukey's multiple comparisons test was employed. In the instance of paired groups (neurons in ACM; e.g., Hn treated with HACM or PDACM), a ratio paired t-test was used to determine the fold changes between pairs. All data are presented as mean ± standard error of the mean (SEM), when samples were normally distributed. Otherwise, the data are presented as medians with interquartile range. Statistical analysis was performed in GraphPad Prism (8.4.3). Probability values smaller than 0.05 ($p < 0.05$) were considered significant.

**Table 1.** Summary of patient-derived cell lines used in this study

| Individual | iPSC lines | Age of skin biopsy | Genotype | Sex | Source/reference |
|---|---|---|---|---|---|
| **Healthy** | H1 | 41 | Wild Type SNCA | M | (Kouroupi et al., 2017) |
| **Healthy** | H2 | 45 | Wild Type SNCA | M | New York Stem Cell Foundation |
| **Patient** | PD1 | 49 | G209A SNCA mutation | M | (Kouroupi et al., 2017) |
| **Patient** | PD2 | 40 | G209A SNCA mutation | M | (Kouroupi et al., 2017) |
| **Patient** | PD3 | 49 | G209A SNCA mutation | F | (Soldner et al., 2011) |
| **Patient (isogenic control)** | $PD3^{corr}$ | 49 | G209A SNCA corrected | F | (Soldner et al., 2011) |

**Table 2.** Reagents used in cell cultures

| REAGENTS | COMPANY | CAT. No |
|---|---|---|
| **Neurobasal™ Medium** | Thermofisher Scientific | 21103-049 |
| **B-27™ Supplement (50X), minus vitamin A** | Thermofisher Scientific | 12587-010 |
| **GlutaMAX (100X)** | Thermofisher Scientific | 35050-038 |
| **Recombinant Human FGF-basic (146 a.a.) 100 µg** | Peprotech | 100-18C-0100 |
| **PeproGMP® Recombinant Human EGF 100 µg** | Peprotech | GMP100-15 |
| **Y-27632 dihydrochloride (ROCK inhibitor) 10 mg** | Tocris | 1254 |

| | | |
|---|---|---|
| **Astrocyte Medium** | Sciencell | 1801 |
| **Advanced DMEM/F12** | Thermofisher Scientific | 12634010 |
| **N-2 Supplement (100X)** | Thermofisher Scientific | 17502-048 |
| **MEM Non-Essential Amino Acids Solution (100X)** | Thermofisher Scientific | 11140-035 |
| **Recombinant Human CNTF 20 µg** | Peprotech | 450-13 |
| **Animal-Free Recombinant Human BMP-4 (E.coli derived) 10 µg** | Peprotech | AF-120-05ET |
| **B-27™ Plus Supplement (50X)** | Thermofisher Scientific | A3582801 |
| **Recombinant Human BDNF Protein, CF, 25 µg** | R&D Systems | 248-BD-025 |
| **Recombinant Human GDNF, 50 µg** | Peprotech | 450-10-50µG |
| **Dibutyryl cyclic-AMP sodium salt** | Sigma Aldrich | D0627 |
| **L-Ascorbic acid (100 mg)** | Sigma Aldrich | A4403 |
| **Recombinant Human TGF Beta 3, 2 µg** | Peprotech | 100-36E |
| **DAPT (N-[2S-(3,5-difluorophenyl)acetyl]-L-alanyl-2-phenyl-glycine, 1,1-dimethylethyl ester)** | Cayman | 13197.10mg |
| **DMEM** | Thermo Fisher Scientific | 11965-092 |
| **HAM's F12** | Thermofisher Scientific | 21765-029 |
| **PBS, pH 7.4, No Calcium, No Magnesium** | Invitrogen | 10010-015 |
| **StemPro® Accutase** | Thermofisher Scientific | A1110501 |
| **Penicillin/Streptomycin** | Thermofisher Scientific | 15140-122 |
| **HEPES 1M** | Thermofisher Scientific | 15630-106 |
| **Geltrex LDEV FREE HESC QUAL** | Thermofisher Scientific | A1413302 |
| **Laminin from Engelbreth-Holm-Swarm murine sarcoma basement membrane** | Sigma | L2020- 1 mg |
| **Poly-l-ornithine hydrobromide (50 mg or 100 mg)** | Sigma | P3655 |
| **Fetal Bovine Serum (FBS)** | Thermofisher Scientific | 10270-106 |

**Table 3.** Primary Antibodies

| NAME | MANUFACTURER, CAT No | DILUTION | BLOCKING | TYPE OF CELLS |
|---|---|---|---|---|
| **α-Synuclein** | BD, 610787 | 1/500 | 5%NDS, 0.3% Triton X-100 in PBS (30 min) | Neurons |

| | | | | |
|---|---|---|---|---|
| **alpha synuclein [MJFR-14-6-4-2]** | Abcam, ab209538 | 1/20000 | 5%NDS, 0.3% Triton X-100 in PBS (30 min) | Neurons |
| **TH** | Millipore, AB152 | 1/500 | 5%NDS, 0.3% Triton X-100 in PBS (30 min) | Neurons |
| **MAP-2** | Synaptic Systems, 188004 | 1/1000 | 5%NDS, 0.3% Triton X-100 in PBS (30 min) | Neurons |
| **CD44** | Cell signaling, 5640S | 1/1000 | 5%NDS in PBS (30 min) | Astrocytes |
| **CD49F** | Biolegend, 313602 | 1/200 | 5%NDS in PBS (30 min) | Astrocytes |
| **GFAP** | DAKO, Z0334 | 1/1000 | 5%NDS in PBS (30 min) | Astrocytes |
| **S100B** | Abcam, Ab41548 | 1/1000 | 5%NDS, 0.3% Triton X-100 in PBS (30min) | Astrocytes |
| **AQP4** | Euroimmun, 1128-0101 | - | 5%NDS in PBS (30 min) | Astrocytes |
| **ALDH1L1** | Abcam, Ab87117 | 1/100 | 5%NDS in PBS (30 min) | Astrocytes |
| **alpha Synuclein (phosphorylated Ser129)** | WAKO, 015-25191 | 1/2000 | 5%NDS in PBS (30 min) | Astrocytes |
| **Rab7** | Cell signalling, 9367 | 1/200 | 5%NDS in PBS (30 min) | Astrocytes |
| **Vimentin** | Synaptic Systems, 172006 | 1/500 | 5%NDS in PBS (30 min) | Astrocytes |
| **FOXA2** | Santa Cruz Biotechnology, sc-101060 | 1/100 | 5%NDS, 0.3% Triton X-100 in PBS (30 min) | NPCs |
| **NESTIN** | Millipore, ABD69 | 1/1000 | 5%NDS, 0.3% Triton X-100 in PBS (30 min) | NPCs |
| **LMX1A** | Millipore, AB10533 | 1/2000 | 5%NDS, 0.3% Triton X-100 in PBS (30 min) | NPCs |
| **PAX6** | Developmental Studies Hybridoma Bank | 1/50 | 5%NDS, 0.3% Triton X-100 in PBS (30 min) | NPCs |

## Results

### Generation and quality control of iPSC-derived ventral midbrain neural progenitors

PD primarily affects the ventral midbrain, especially the dopaminergic neurons in the ventrolateral substantia nigra (Poewe et al., 2017). To generate iPSC-derived ventral midbrain neural progenitor cells (NPCs), we utilized a protocol established by (Kriks et al., 2011), with modifications, that provided expandable floor plate neural progenitors that could be differentiated into both neurons and astrocytes of the ventral midbrain (de Rus Jacquet, 2019) (Fig. 1a). The protocol relies on the inhibition of BMP (Bone Morphogenic Protein) and TGFβ (Transforming Growth Factor beta) signaling pathways. Most importantly, the protocol is based on the fact that the floor plate-derived signal sonic hedgehog (SHH) is required for the induction of ventral midbrain dopaminergic neurons during embryogenesis (Kriks et al., 2011). The successful regionalization of NPCs was confirmed by the high abundance of $FOXA2^+$ cells (floorplate marker) and $LMX1A^+$ cells (midbrain marker), and low abundance of $PAX6^+$ cells (roofplate marker) in double immunostainings with Nestin (Fig. 1b). Moreover, by RT-qPCR we verified the relative upregulation of floorplate- and midbrain-specific gene expression relative to roofplate-, caudal-, and rostral- specific genes (not shown). Only properly patterned NPCs were used in subsequent experiments after their expansion for 2 to 3 passages, to which point they are used for subsequent differentiation to ventral midbrain dopaminergic neurons (vmDAn) (Fig. 3a) or for at least 4 weeks for subsequent astrocytic differentiation (Fig. 2a).

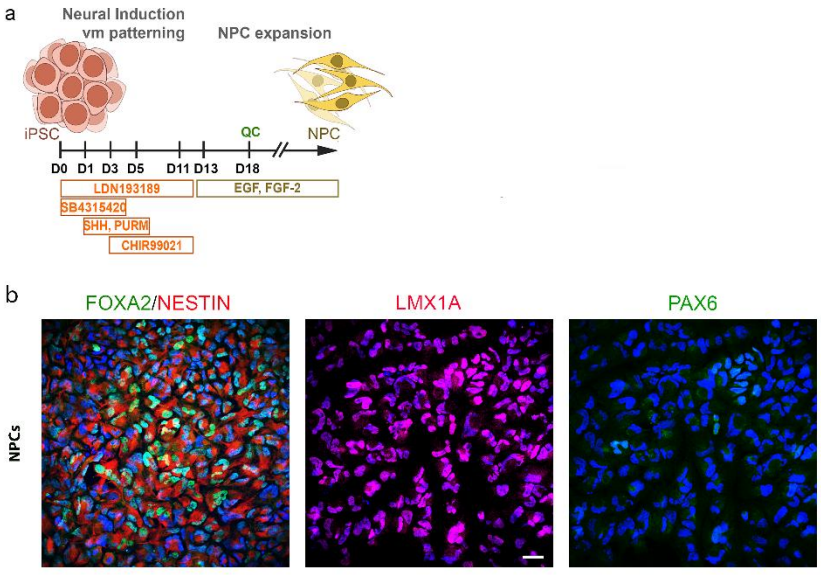

**Figure 1. Protocol outline and quality control of NPCs| a.** Graphical outline of the protocol applied for neural induction/ventral midbrain patterning towards floor plate progenitors. "D" indicates the days from the beginning of neural induction. **b.** Representative confocal images of NPCs immunostained for midbrain/floorplate markers: FOXA2 (green)/Nestin (NPC marker; red), LMX1A (red), and roof plate marker PAX-6 (green) with DAPI nuclear counterstain (blue). Scale bar, 30 µm.

*DAPI, 4',6-diamidino-2-phenylindole; FOXA2, Forkhead box A2; LMX1A, LIM homeobox transcription factor 1 alpha; NPC, neural precursor cell; PAX-6, Paired box protein 6.*

## Generation of iPSC-derived ventral midbrain iAstrocytes

Given the regional diversity of astrocytes (Kostuk et al., 2019), to establish a PD-relevant *in vitro* model, we generated ventral midbrain-regionalized astrocytes from patient-derived iPSCs by adopting established protocols (de Rus Jacquet, 2019; Kriks et al., 2011) (Fig. 2a). After 28 days of differentiation at low plating density in Astrocyte Medium, both healthy and PD iPSC-derived astrocytes (iAstrocytes, hereafter referred to as Ha and PDa, respectively) displayed robust expression of markers of the astroglial fate, including CD44, vimentin, Aldehyde Dehydrogenase 1 Family Member L1 (ALDH1L1), and S100β (Fig 2b). No differences were apparent in the differentiation potential and morphology between Ha and PDa (Fig. 2b). More mature astrocytic markers including aquaporin 4 (AQP4), Excitatory amino acid transporter 1 (EAAT1), and CD49f were enriched after a 2-week maturation treatment with bone morphogenetic protein-4 (BMP-4) and ciliary neurotrophic factor (CNTF) (Fig. 2c). Unless otherwise stated, in the downstream analyses we assayed iAstrocytes after the end of the differentiation stage (after d28, Fig. 2a), to avoid interference from BMP4 (transforming growth factor-beta superfamily member) and CNTF (interleukin-6 [IL-6] subfamily member) to the astrocytic reactivity state (Sofroniew, 2009).

Title: Astrocyte Dysfunction in Parkinson's Disease: Insights from Neuron-Astrocyte Interactions in a Patient-Derived Model
Student Name: Sofia Dede

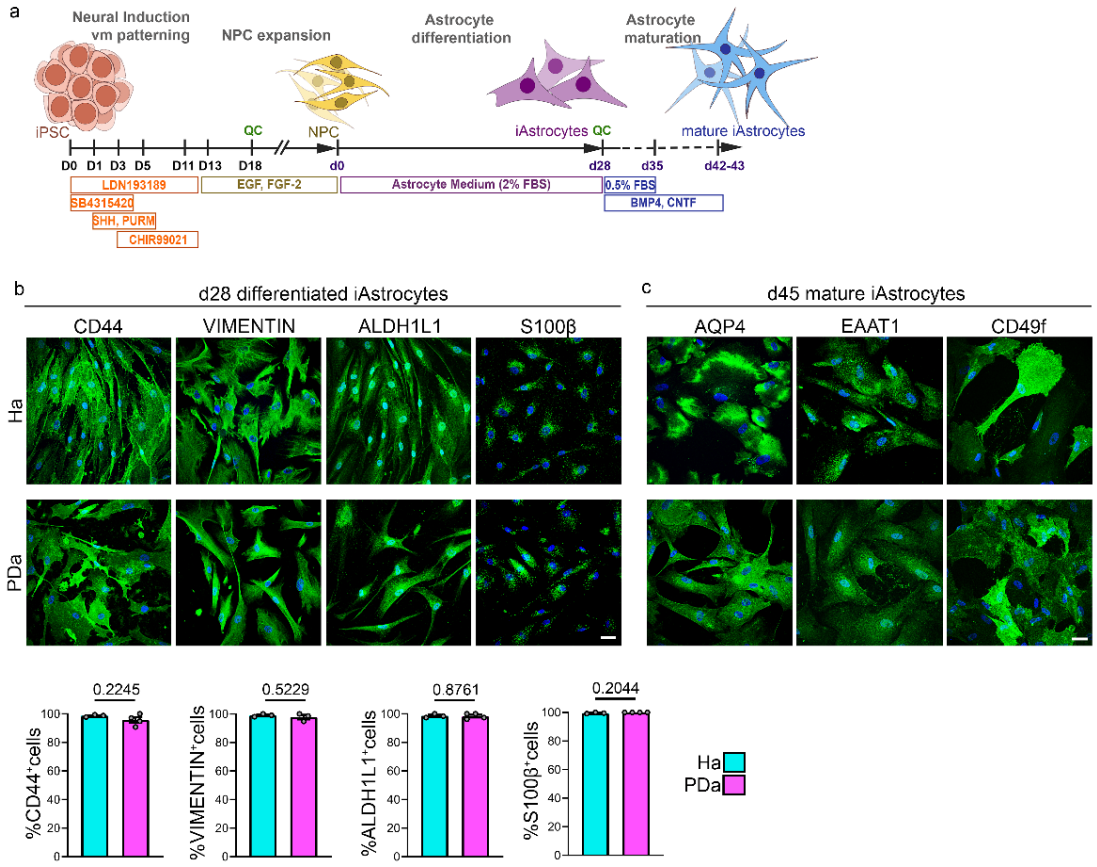


**Figure 2. Generation of iPSC-derived ventral midbrain iAstrocytes | a.** Graphical outline of the protocols applied for neural induction/patterning, NPCs generation, and astrocyte differentiation, followed by astrocyte maturation. "D" indicates the days from the beginning of neural induction and "d" days of astrocyte differentiation **b.** Representative confocal image of iPSC-derived astrocytes, after 28 d of differentiation, showing expression of typical astrocytic markers CD44, Vimentin, ALDH1L1, and S100β. Bar plots depict the quantification of the percentage of cells expressing each marker relative to the total cell population (DAPI). **c.** Representative confocal images of iPSC-derived astrocytes after 28 d of differentiation, followed by an additional 15 d of maturation, showing expression of more mature astrocytic markers: AQP4, EAAT1, and CD49f. Scale bars: 40 µm. Data are presented as mean ± SEM; Unpaired two-tailed t-test was used for comparisons; Sample sizes: n = 3 Ha and n = 4 PDa independent non-isogenic lines.

*AQP4, Aquaporin-4; CD44, Cluster of Differentiation 44; CD49f, Integrin alpha-6; DAPI, 4',6-diamidino-2-phenylindole; EAAT1, Excitatory amino acid transporter 1; Ha, healthy astrocytes; PDa, p.A53T-αSyn astrocytes; S100β, S100 calcium-binding protein B; Vimentin, intermediate filament protein; SEM, standard error of the mean.*

## Generation of iPSC-derived ventral midbrain dopaminergic neurons

In previous works from our lab, PD neurons from p.A53T-αSyn iPSCs were characterized in detail (Antoniou et al., 2022; Kouroupi et al., 2017; Zygogianni et al., 2019). Here, we generated vmDAn from the same populations of iPSCs, as for the astrocytic differentiation, by adopting established protocols (de Rus Jacquet, 2019; Kriks et al., 2011) (Fig. 3a). Immunofluorescence was performed at 28 days of neuronal differentiation (NDIV) to test the expression of tyrosine hydroxylase (TH) in iPSC-derived vmDAn. TH is considered an essential marker of the dopaminergic fate (Grigor'eva et al., 2023). Both healthy and PD microtubule-associated protein 2$^{+}$ (MAP2$^{+}$) neurons were positive for TH at a high percentage (Fig. 3b).

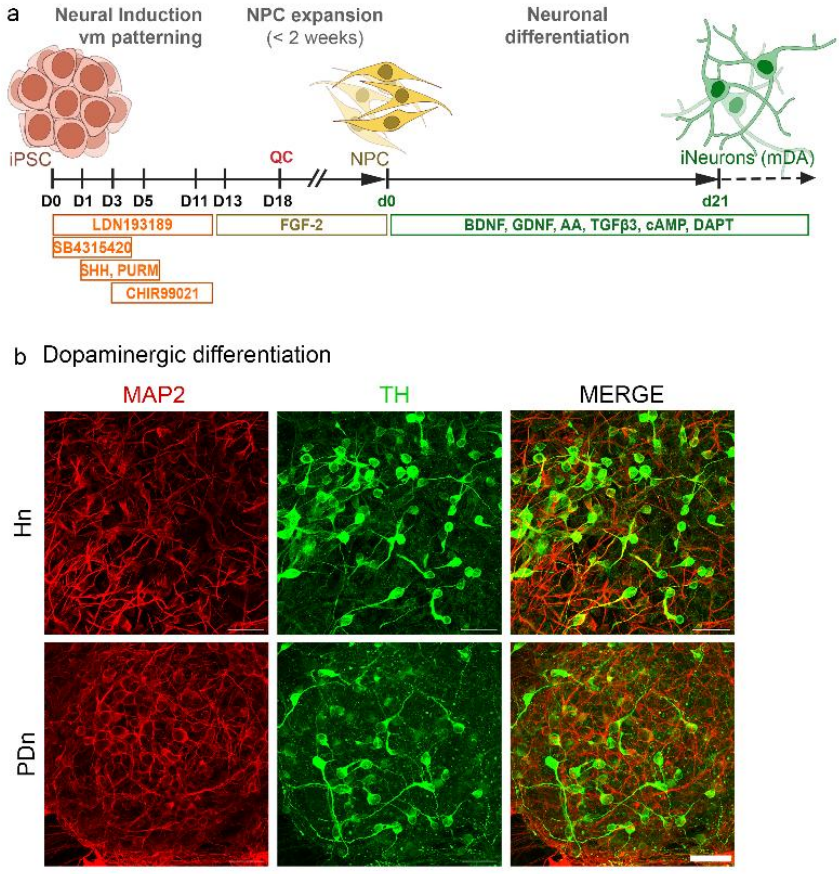


**Figure 3. Establishment of dopaminergic identity of iPSC-derived neurons | a.** Graphical outline of the protocol applied for neural induction/patterning, NPCs generation, and neuronal differentiation. "D" indicates the days from the beginning of neural induction and "d" days of neuronal differentiation. **b.** Representative images of TH$^{+}$ vmDAns in Hn and PDn at NDIV28. Scale bars: 30 µm.

*MAP2, Microtubule-associated protein 2; TH, tyrosine hydroxylase; PDn, p.A53T-αSyn neurons; Hn, healthy neurons; vmDAn, ventral midbrain dopaminergic neurons.*

## The p.A53T-αSyn mutation affects Tunneling Nanotubes (TNTs) biogenesis in astrocytes

Unpublished data of our lab showed that Ha alleviated PD-relevant neuropathology including Lewy-like p(Ser129)αSyn$^{+}$ structures in p.A53T-αSyn iNeurons (PDn) in a co-culture system (Paschou, Apokotou et al., under submission). However, the underlying mechanisms are still under examination. Tunneling nanotubes (TNTs) have emerged as pivotal structures for intercellular communication, enabling the transfer of cellular components across distant cells. TNTs are reported as conduits for the direct transfer of αSyn aggregates between brain cells and are involved in spreading of neurodegenerative pathologies and PD (Abounit et al., 2016; Chakraborty et al., 2023; Loria et al., 2017; Rostami et al., 2017a). We investigated whether our iPSC-derived astrocytes are able to form TNTs in control conditions. The membrane (WGA) and F-Actin (Phalloidin) were labeled in differentiation day-38 Ha and PDa and showed that under normal culture conditions, iPSC-derived astrocytes formed TNT-like structures. The number of TNT-connected cells was significantly increased among astrocytes carrying the p.A53T-αSyn mutation, compared to Ha (Fig. 4a, c). Moreover, the number of TNT-connections per cell was significantly increased in PDa, compared to Ha (Fig. 4c). Subsequently, we assessed the number of TNTs after 16-h treatment of astrocytes with human αSyn pre-formed fibrils (PFFs) conjugated with AlexaFluor-568. The number of TNT-connections per cell was significantly increased in both Ha and PDa after PFF treatment compared to non-treated cells, while the number of TNT-connected cells significantly increased only in the case of Ha, after the treatment (Fig. 4b, c). Moreover, after treatment, PDa displayed significantly increased number of TNT-connected cells and TNTs per cell, as compared to Ha (Fig. 4c). The above results indicate that the p.A53T-αSyn mutation and PFF treatment cause an increase in the biogenesis of TNT-like structures in astrocytes.

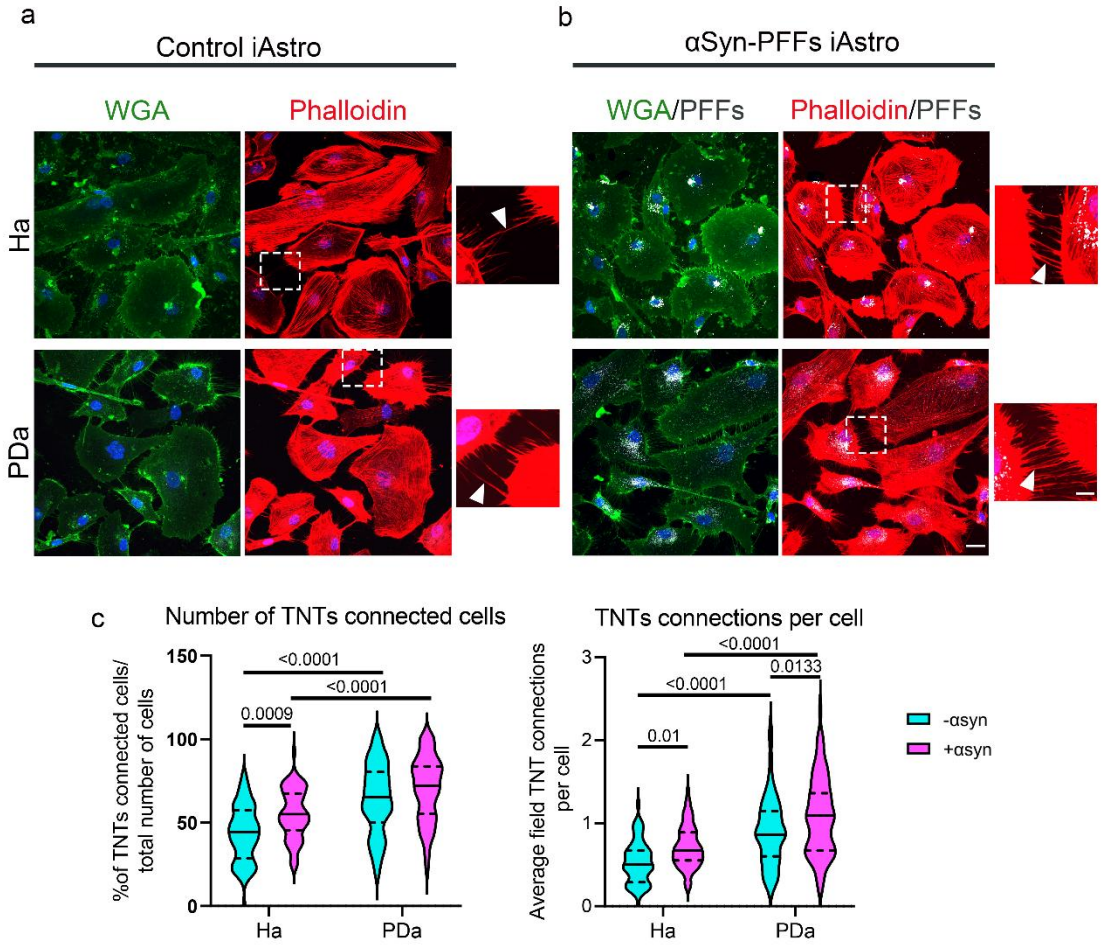


**Figure 4. Increased formation of TNTs by p.A53T-αSyn Astrocytes| a.** Representative confocal images of Ha and PDa under normal growth conditions labeled with AlexaFluor647 WGA (green) and AlexaFluor488 Phalloidin (red). Magnifications of the boxed areas are shown in insets. Full arrowheads indicate TNTs-like structures. Scale bar: 30 µm. **b.** Representative confocal images of Ha and PDa after 16-h treatment with αSyn-PFF-AlexaFluor568 (white) labeled with AlexaFluor647 WGA (green) and AlexaFluor488 Phalloidin (red). Magnifications of the boxed areas are shown in insets. Full arrowheads indicate TNTs-like structures. Scale bar: 30 µm. Scale bar, inset: 10 µm **c.** Violin plots showing the distributions of %TNT-connected cells over the total number of cells and the number of the average TNT-connections per cell in Ha and PDa before and after the treatment with PFFs. Data are presented as median with interquartile range. Two-way ANOVA with Tukey's multiple comparisons test was employed. Sample sizes: n = 3 Ha and n = 3 PDa independent lines (including the isogenic pair) from separate experiments.

*TNTs, Tunneling nanotubes; Ha, healthy astrocytes; PDa, p.A53T-αSyn astrocytes; αSyn-PFF, α-synuclein pre-formed fibrils; WGA, Wheat Germ Agglutinin.*

## Deficient uptake of exogenous p(Ser129)αSyn$^{+}$ cargo by p.A53T-αSyn Astrocytes

The ability of astrocytes to internalize and degrade αSyn, preserving neuronal health status, has been highlighted previously (Braidy et al., 2013; Rostami et al., 2017b; Tsunemi et al., 2020). Additionally, we have shown that PDa express reduced phagocytic activity when exposed to pHRodo-*E. coli* bioparticles (Paschou, Apokotou

et al., under submission). Here we tested the ability of our iAstrocytes to efficiently uptake neuronal αSyn. To address that, we treated mature Ha and PDa with medium conditioned by d21 iNeurons carrying the p.A53T-αSyn mutation (PDnCM) for 48 h (Fig. 5a). PDn are expected to exocytose a mixture of αSyn species, including monomers, oligomers, and potentially fibrils, in the extracellular space (Emmanouilidou et al., 2010b; Stykel et al., 2021), i.e., in the culture medium in our setup. After a 6-h treatment with PDnCM, we measured the number of p(Ser129)αSyn immunopositive puncta (round spots) per cell, relatively to the numbers before treatment, and found a marked increase in Ha and a significantly lower increase in PDa (Fig. 5b,c). These puncta presumably represent uptaken αSyn, found in its phosphorylated form in the PDnCM, captured at different stages of the endo-lysosomal pathway. Interestingly, some of these p(Ser129)αSyn$^{+}$ puncta were co-localized with Rab7 (early-to-late endosome marker) (Fig. 5b), responsible for αSyn sorting for degradation via lysosomes and reduction of intracellular accumulation of αSyn (Masaracchia et al., 2018). To discriminate between the assumed uptaken p(Ser129)αSyn from the endogenous p(Ser129)αSyn aggregates previously observed accumulating in PDa at steady state in our lab (Paschou, Apokotou et al., under submission), we compared the circularity of p(Ser129)αSyn puncta in Ha after PDnCM treatment and in untreated (control) PDa. In Ha, the p(Ser129)αSyn puncta were significantly more circular (as expected for cargo encapsulated in vesicles) than those in PDa, which were rather irregularly shaped (Fig. 5b,d). To exclude an induced up-regulation of SNCA gene expression in PDnCM-treated Ha, we determined the SNCA mRNA levels by RT-qPCR before and after PDnCM treatment and found no significant differences (Fig. 5e). These data indicate an inherent inability of p.A53T-αSyn astrocytes to properly uptake neuronal pS129aSyn.

Title: Astrocyte Dysfunction in Parkinson's Disease: Insights from Neuron-Astrocyte Interactions in a Patient-Derived Model
Student Name: Sofia Dede

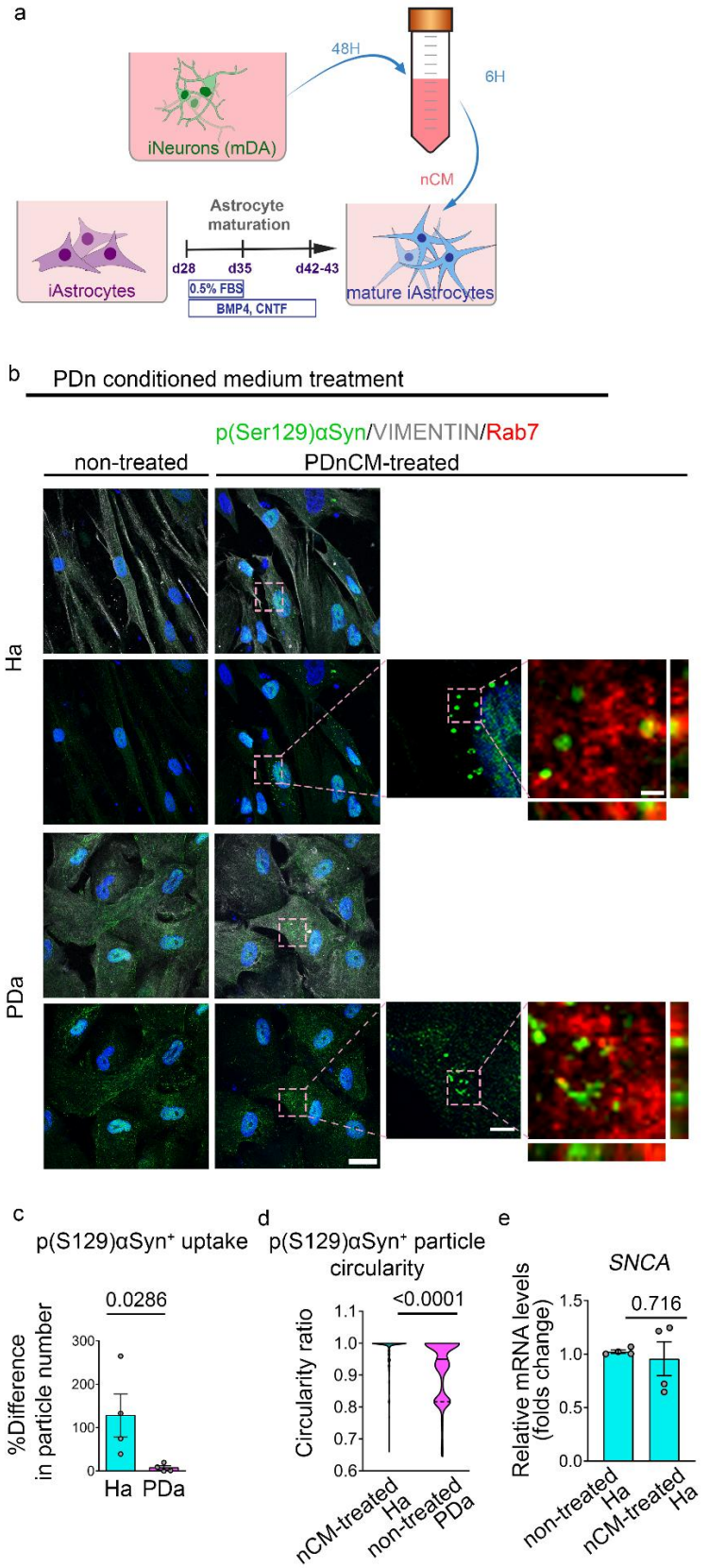


**Figure 5. Impaired uptake of neuronal αSyn by p.A53T-αSyn Astrocytes| a.** Schematic overview of the protocol used for the treatment of iAstrocytes with neuronal conditioned medium (nCM). **b.**

Representative confocal images of mature Ha and PDa, both untreated and 6 h after PDnCM treatment. Cells were immunostained for p(S129)αSyn, Vimentin, and Rab7. Scale bars: 30 µm, 4 µm (middle insets), and 1 µm (right insets). Orthogonal sectioning of p(S129)αSyn$^{+}$ puncta with Rab7 colocalization. **c.** Bar plot showing the quantification of the percentage difference in the number of p(Ser129)αSyn+ puncta in Ha and PDa after PDnCM treatment, relative to the corresponding measurement before treatment. **d.** Violin plot showing the distribution of the circularity of cytoplasmic p(Ser129)αSyn$^{+}$ particles found in Ha after PDnCM treatment and in untreated PDa. **e.** Bar plot representing the relative mRNA levels of SNCA gene normalized to GAPDH in non-treated Ha and PDnCM-treated Ha. Data are presented as mean ± SEM (c, e) or as median with interquartile range (d); For statistical comparisons, unpaired two-tailed t-test test was used in c, paired two-tailed t-test in e and Kolmogorov-Smirnov test was used to compare distributions in d; Sample sizes: c, n = 4 Ha and n = 4 PDa independent lines (including the isogenic pair); d, n = 704 particles from nCM-treated Ha and n = 268 particles from non-treated PDa, across 4 independent Ha lines and 4 independent PDa lines (including the isogenic pair); e, n = 4 independent Ha lines (including the PD3$^{corr}$a line); all from independent experiments (c-e).

*Ha, healthy astrocytes; PDa, p.A53T-αSyn astrocytes; PD3corra, isogenic control; nCM, neuronal conditioned medium; p(Ser129)αSyn, phosphorylated α-synuclein at Serine 129; Rab7, Ras-related protein 7; SEM, standard error of the mean; SNCA, α-synuclein gene.*

## Deficient processing of exogenous αSyn pre-formed fibrils (PFFs) by p.A53T-αSyn Astrocytes

Subsequently, we tested the ability of p.A53T-αSyn mutant astrocytes to endocytose and degrade αSyn aggregates in a different and more controlled setup. We treated d38 Ha and PDa with recombinant αSyn pre-formed fibrils (αSyn-PFFs) conjugated with Alexa 568 and observed the kinetics of αSyn-PFF endocytosis through the time points of 1, 2, 4, 6, and 16 h. At the early time points (1 and 2 h), there was no significant difference between internalized αSyn-PFFs by Ha and PDa. At longer time points (4 and 6 h) αSyn-PFFs accumulated in the cytoplasm of PDa, as compared to Ha, reaching significance at 16 h (Fig. 6a, b), pointing toward a retarded degradation process. To further empower this hypothesis, we repeated the same experiment only for the 16-h time-point but this time free αSyn-PFFs were washed away from the cultures after 2 h of treatment, by medium change, to count out the bias from cumulative uptake during the 16-h time-course that may interfere with degradation rates. The results from this experiment showed again that at the 16-h time-point the αSyn-PFFs were significantly more accumulated in the cytoplasm of PDa, as compared to Ha, verifying the clearance lag (Fig 6c). The higher-order species of αSyn

in the PFFs are considered much more pervasive due to their stability and resistance to degradation (Luk et al., 2009), contrary to the more heterogeneous and dynamic mixture of αSyn species expected to be present in PDnCM, reflecting the complex environment of the PD brain. We presume that the difference between the kinetics after treatment with PDnCM (6 h corresponding to simultaneous uptake and degradation) and αSyn-PFFs (6 h and onwards reflecting accumulation of already uptaken fibrils), is explained by the relatively high and stable concentration of the added PFFs (as compared with the secreted αSyn in PDnCM).

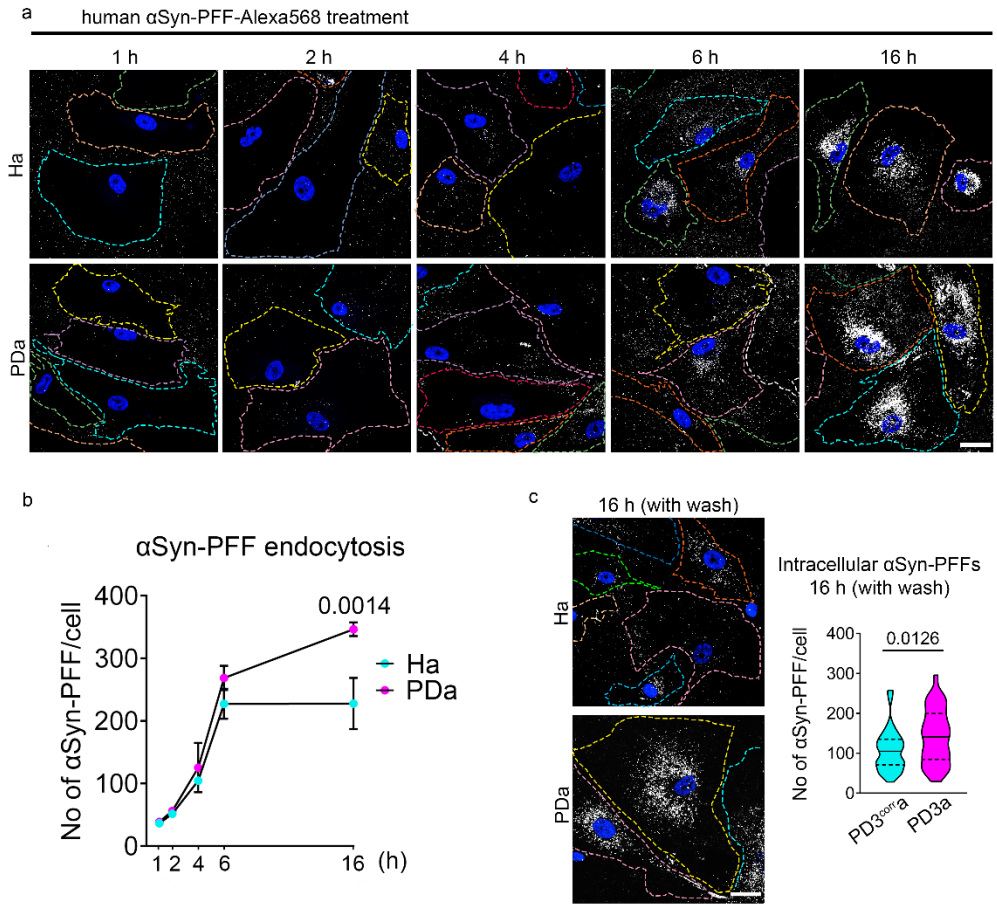


**Figure 6. Impaired processing of αSyn pre-formed fibrils by p.A53T-αSyn Astrocytes| a.** Representative confocal images of Ha and PDa at 1, 2, 4, 6, and 16 h after treatment with αSyn-PFF-AlexaFluor568 (white). Randomly-colored dashed lines demarcate cell borders. Scale bar: 30 µm. **b.** Line graph illustrating the time course of intracellular processing of the uptaken αSyn-PFF-Alexa568 in Ha and PDa. **c.** Representative confocal images of PD3$^{corr}$a and PD3a at 16 h after a 2-h αSyn-PFF-Alexa568 treatment followed by washout and violin plot with quantification of intracellularly detected αSyn-PFFs. Scale bar: 30 µm. Data are presented as mean ± SEM (b) or as median with interquartile range (c). Two-way ANOVA with Sidak post-hoc analysis for multiple comparisons was used in b, and

Mann-Whitney tests were used for comparisons in c. Sample sizes: b, n = 3 Ha or PDa lines (including the isogenic pair) from separate experiments; c, n = 36 $PD3^{corr}a$ and 43 PD3a cells.

*αSyn-PFF, α-synuclein pre-formed fibrils; Ha, healthy astrocytes; PDa, p.A53T-αSyn astrocytes; PD3corra, isogenic control; PD3a, p.A53T-αSyn astrocytes; SEM, standard error of the mean.*

## PFF-loaded neuronal cells co-cultured with healthy astrocytes display enhanced clearance of αSyn-PFFs

Our next objective was to explore whether the observed uptake/clearance deficits in PDa affect their capacity to facilitate the clearance of neuronal cells from αSyn aggregates. We exposed GFP-tagged SH-SY5Y human neuroblastoma cells to αSyn-PFFs for 16 h and then the neuroblastoma cells were dissociated, mixed with either Ha or PDa, and plated for an additional 24 h (Fig. 7a). Confocal analysis at the end point demonstrated that the SH-SY5Y cells co-cultured with PDa harbored significantly more intracellular αSyn-PFFs, compared to those co-cultured with Ha (Fig. 7b). Likewise, the PDa co-cultured with αSyn-PFF-loaded SH-SY5Y cells contained significantly more αSyn-PFFs, as compared to Ha also co-cultured with αSyn-PFF-loaded SH-SY5Y cells (Fig. 7c). Collectively, these findings suggest that astrocytes carrying the p.A53T-αSyn mutation display inherent deficiencies in their uptake and protein aggregate degradation properties, and thus are less capable of relieving neuronal cells from accumulated αSyn (Paschou, Apokotou et al., under submission).

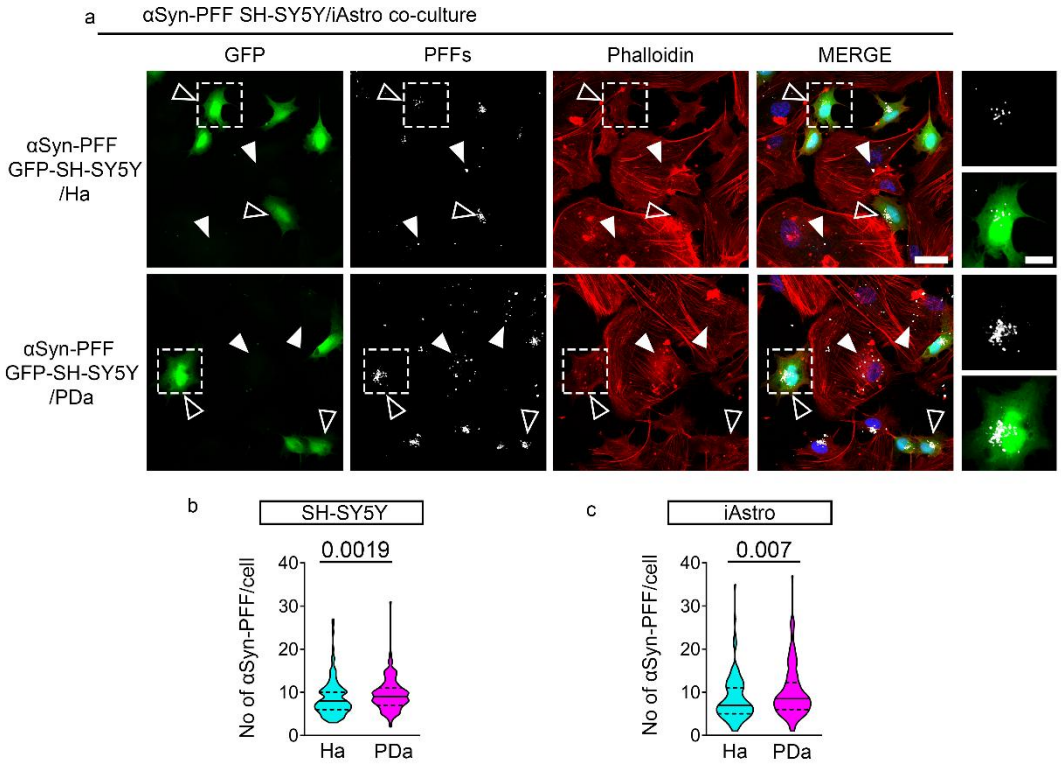


**Figure 7. Enhanced clearance of αSyn-PFFs in PFF-loaded SHSY-5Y cells co-cultured with Ha| a.** Representative confocal images of Ha and PDa co-cultured for 24 h with GFP-SH-SY5Y neuroblastoma cells loaded with αSyn-PFF-AlexaFluor568 (white), labeled with AlexaFluor647 Phalloidin (red). Magnifications of the boxed areas are shown in insets. Empty arrowheads indicate αSyn-PFFs in GFP-SH-SY5Y cells; full arrowheads indicate αSyn-PFFs in iAstrocytes. Scale bar: 30 µm. Scale bar insert: 5µm. **b.** Violin plot showing the distribution of the numbers of αSyn-PFFs per cell in GFP-SH-SY5Y cells, after 24 h in co-culture with either Ha or PDa. **c.** Violin plot showing the distribution of the numbers of αSyn-PFFs per cell in Ha and PDa after 24 h in co-culture with αSyn-PFF-loaded GFP-SH-SY5Y cells. Data are presented as median with interquartile range. Mann-Whitney tests were used. Sample sizes: b, n = 154 GFP-SH-SY5Y cells (co-cultured with 3 independent Ha lines) and n = 154 GFP-SH-SY5Y cells (co-cultured with 3 independent PDa lines) from separate experiments (including the isogenic pair); c, n = 145 cells (Ha) and n = 147 cells (PDa), across 3 Ha and 3 PDa independent lines (including the isogenic pair) from separate experiments.

*αSyn-PFF, α-synuclein pre-formed fibrils; Ha, healthy astrocytes; PDa, p.A53T-αSyn astrocytes; GFP, Green Fluorescent Protein.*

## The p.A53T-αSyn mutation affects lysosomal physiology in astrocytes

Comparative proteomic analysis of PDa and Ha performed in our lab implicates lysosomal proteins (Paschou, Apokotou et al., under submission). Alongside the observed phenotypes, these data led us to examine lysosomal integrity in PDa. We used Lysotracker DR to label live cells and we recorded increased number of

lysosomes that may reflect reduced consumption of lysosomes due to impaired autophagy or a compensatory response to lysosomal dysfunction (Mutvei et al., 2023). Additionally, the fluorescence intensity of Lysotracker DR was lower in PDa than in Ha, indicative of reduced acidity (Fig. 8a). Notably, defective lysosomal acidification has been implicated as a key driving factor in the pathogenesis of NDD, including AD and PD (Lo & Zeng, 2023). Using the pH-sensitive fluorescent dye Lysosensor Green, we confirmed the significant decrease of lysosomal acidity in PDa (Fig. 8b). The assessment of Cathepsin B lysosomal enzyme pH-dependent activity, using the Magic Red kit, revealed reduced activity in PDa as compared to Ha (Fig. 8c). The above results demonstrate that defective lysosomal properties in the PD iAstrocytes may account for the dysfunctional autophagic flux, and protein aggregate accumulation noted and described in our under-submission manuscript Paschou, Apokotou et al.

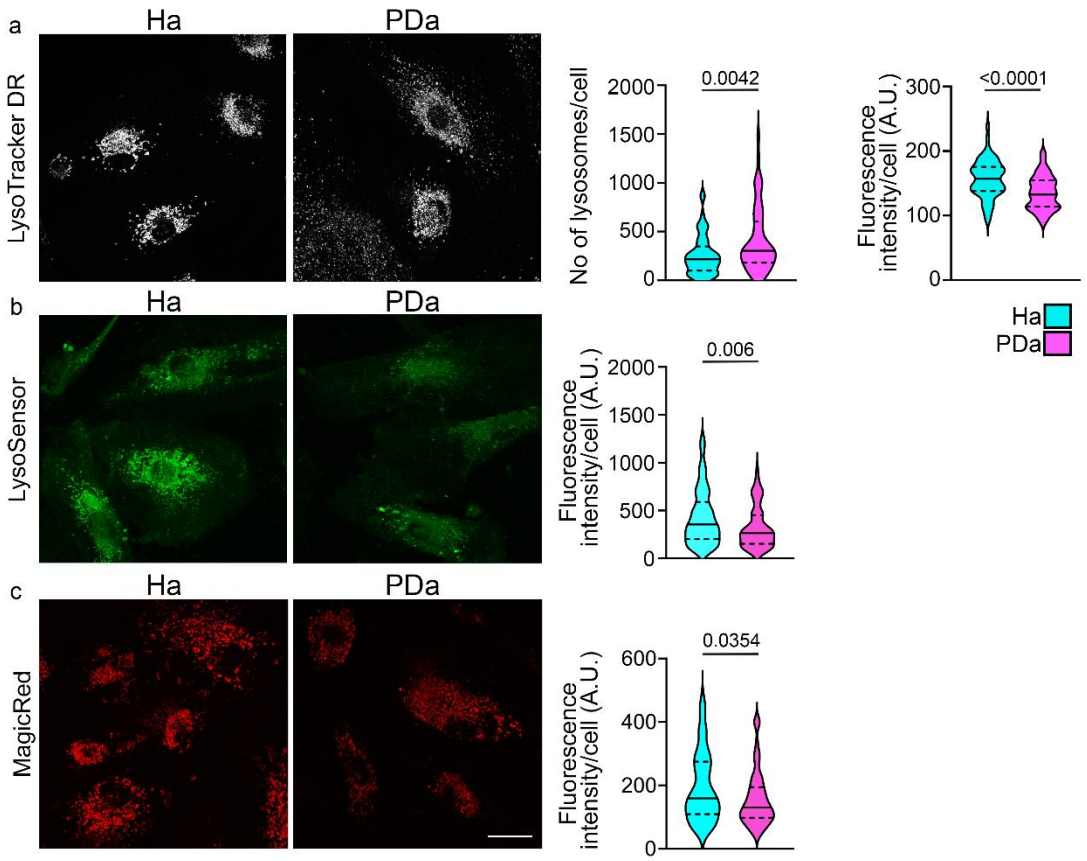


**Figure 8. Lysosomal malfunction in astrocytes with the p.A53T-αSyn mutation| a.** Representative images and quantification of live Ha and PDa after labeling with the fluorescent dye LysoTracker DR. Violin plots show the distributions of lysosome numbers per cell (left) and of the fluorescent

intensities per cell (right). **b, c**. Representative images and quantification of live Ha and PDa after labeling with the pH-sensitive fluorescent dye LysoSensor (b) or Magic Red indicating Cathepsin B activity (c); violin plots show the distribution of fluorescence intensities per cell. Scale bar: 30 µm. Data are presented as median and interquartile range. Mann-Whitney test was performed in all comparisons; Sample sizes: a, n = 60 cells across 3 Ha lines and 60 cells across 3 PDa lines (including the isogenic pair); b, n = 112 cells across 3 Ha and 105 cells across 3 PDa lines (including the isogenic pair); c, n = 74 cells across 3 Ha and 81 cells across 3 PDa lines (including the isogenic pair).

*Ha, healthy astrocytes; PDa, p.A53T-αSyn astrocytes.*

## Healthy astrocytes reduce intraneuronal protein aggregates in PD neurons in a paracrine manner

In a co-culture setup of iPSC-derived neurons and astrocytes we detected a significant reduction in the number of protein aggregates and Lewy-like p(Ser129)αSyn$^{+}$ inclusions in PDn when co-cultured for 14 d with Ha, as compared to being co-cultured with PDa (Paschou, Apokotou et al., under submission). Previous studies demonstrate that astrocytes affect neuronal αSyn-load and its aggregation through their secretome (di Domenico et al., 2019; Yang et al., 2022). These data, along with the aforementioned effect of Ha to enhance the clearance of aggregated αSyn (in the form of PFFs), led us to examine whether mediators secreted by astrocytes are implicated. We treated d21 PDn with astrocyte-conditioned medium (ACM) from mature Ha or PDa (Fig. 9a). After 1 week of treatment with ACM, we found that PDn treated with Ha-conditioned medium (HACM) displayed reduced number of intraneuronal protein aggregates and of αSyn aggregates (trend), as compared to condition media from PDa (Fig. 9b). This suggests that paracrine factors secreted from Ha may facilitate directly or indirectly (e.g., promoting neuronal autophagy) the clearance of protein aggregates and more importantly of αSyn aggregates in PDn, providing neuroprotection. More biological replicates and additional experiments are necessary to corroborate this finding.

Title: Astrocyte Dysfunction in Parkinson's Disease: Insights from Neuron-Astrocyte Interactions in a Patient-Derived Model
Student Name: Sofia Dede

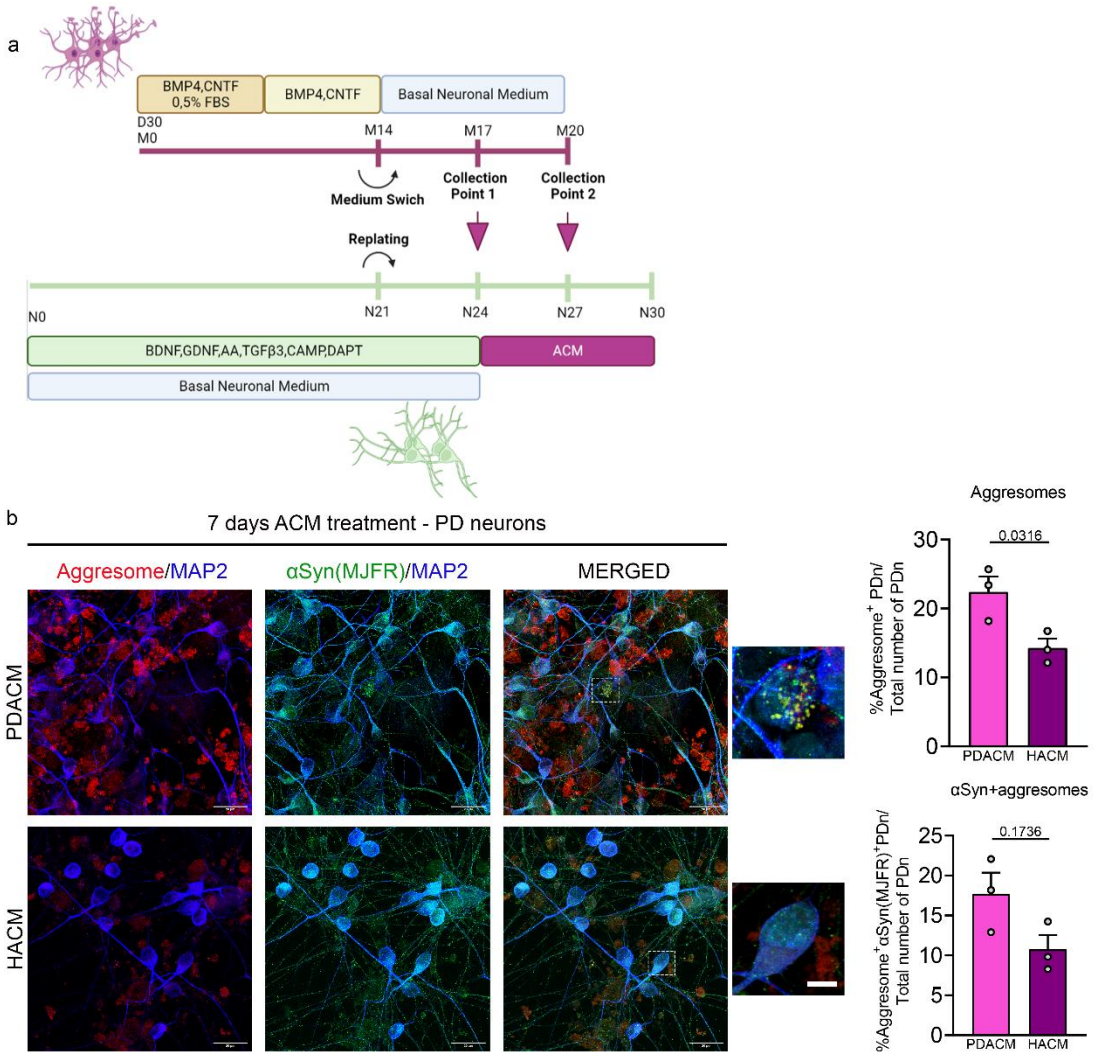


**Figure 9. Decrease of protein aggregates in PDn by Ha-conditioned media |a.** Graphical illustration of the protocol applied for Astrocyte-Conditioned Medium Collection. "D" indicates the days of astrocyte differentiation, "N" the days of neuronal differentiation and "M" the days of astrocyte maturation. **b.** Representative confocal images of PDn after 7-d ACM treatment from PDa or Ha, showing simultaneous Aggresome staining (red) and immunostaining for MAP2 (blue) and αSyn MJFR (green). Scale bar, 20 µm. Magnifications of the boxed areas are shown in insets. Scale bar (inset): 4 µm. Bar plots showing the quantification of the number of PDn with aggregates and PDn with aggregates containing αSyn, relative to the total number of PDn per field, after treatment with ACM from Ha or PDa. Data are presented as mean ± SEM. Ratio-paired t-test was used for comparisons. Sample sizes: n = 3 PDn (including the isogenic pair) from separate experiments.

*ACM, Astrocyte-Conditioned Medium; Ha, healthy astrocytes; Hn, healthy neurons; PDn, p.A53T-αSyn neurons; PDa, p.A53T-αSyn astrocytes; αSyn, alpha-synuclein; MAP2, Microtubule-associated protein 2; SEM, standard error of the mean.*

## PD astrocyte-conditioned medium increases neuronal αSyn levels in healthy neurons

We next questioned whether ACM further affects the levels of total αSyn in iNeurons. We treated healthy neurons (Hn) and PDn with conditioned medium from Ha and PDa at all possible combinations. After 1 week of treatment with ACM, we measured the intensity of αSyn in randomly selected neuronal cell bodies. We found that treatment of Hn with conditioned medium from PDa increased the intensity of αSyn, as compared to that measured after treatment with conditioned medium from Ha (Fig. 10 a,b). This is an indication that astrocytes carrying the p.A53T-αSyn mutation contribute to the neurodegeneration process through there secretome triggering an increase in αSyn-load in Hn. No difference in terms of αSyn intensity was detected in PDn when treated with either healthy or PDACM. More biological replicates are necessary to corroborate this finding.

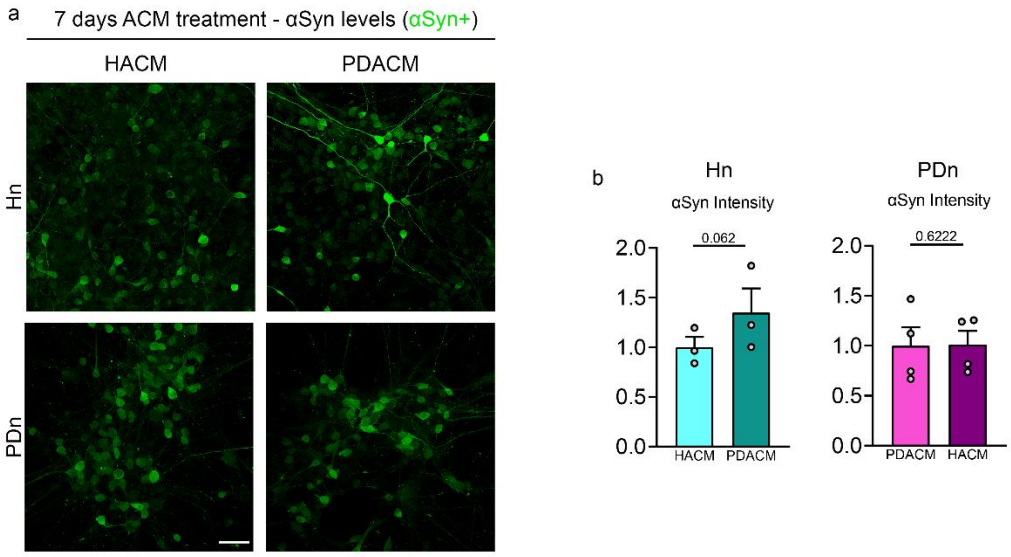


**Figure 10. Increased αSyn-load in Hn by PD astrocyte-conditioned media |a.** Representative confocal images of 7-d treated Hn with HACM or PDACM and PDn with HACM or PDACM, showing immunostaining for total αSyn (green). Scale bar, 30 µm. **b.** Bar plots indicating the quantification of mean intensity of αSyn in Hn and PDn after Ha or PDa ACM treatment. Data are presented as mean ± SEM. Ratio-paired t-test was used for comparisons. Sample sizes: n = 3 Hn and n = 4 PDn (including the isogenic pair) from separate experiments.

*HACM, Healthy Astrocyte-Conditioned Medium; PDACM, PD Astrocyte-Conditioned Medium; Ha, healthy astrocytes; Hn, healthy neurons; PDn, p.A53T-αSyn neurons; PDa, p.A53T-αSyn astrocytes; αSyn, alpha-synuclein; SEM, standard error of the mean.*

## Healthy astrocytes display neuroprotective effect in dopaminergic PD neurons mediated by their secretome

Unpublished data of our lab revealed that total survival and more profoundly the survival of $TH^+$ dopaminergic PDn were increased when co-cultured for 14 days with Ha, as compared to PDa (Paschou, Apokotou et al., under submission). Based on these experiments and on previous publications demonstrating that astrocytes affect neuronal survival in a paracrine manner (Barbar, Jain, et al., 2020; di Domenico et al., 2019; Qiao et al., 2016), we next sought to investigate whether neuronal survival and/or differentiation are influenced by secreted mediators. To this end, Hn and PDn were treated with conditioned medium from Ha and PDa at all possible combinations. After 1 week of treatment with ACM, we assessed total neuronal population (immunostained for MAP2) and the population of dopaminergic neurons (immunopositive for TH). We found that conditioned medium from Ha rescued the population of $TH^+$ dopaminergic PDn, as compared to their compromised survival when treated with ACM from PDa. No difference was detected in total neuronal population (Fig. 11 a,c). In the case of Hn, both total neurons and $TH^+$ dopaminergic neurons were reduced after treatment with conditioned medium from PDa, as compared to their counterparts after ACM from Ha (Fig. 11 a,b). The above results indicate that astrocytes carrying the p.A53T αSyn mutation are potentially neurotoxic and this effect could be non-contact mediated. Further, Ha conditioned medium capacity to rescue dopaminergic PDn indicates a protective effect against dopaminergic neuronal loss mediated at least partially by paracrine mediators.

Title: Astrocyte Dysfunction in Parkinson's Disease: Insights from Neuron-Astrocyte Interactions in a Patient-Derived Model
Student Name: Sofia Dede

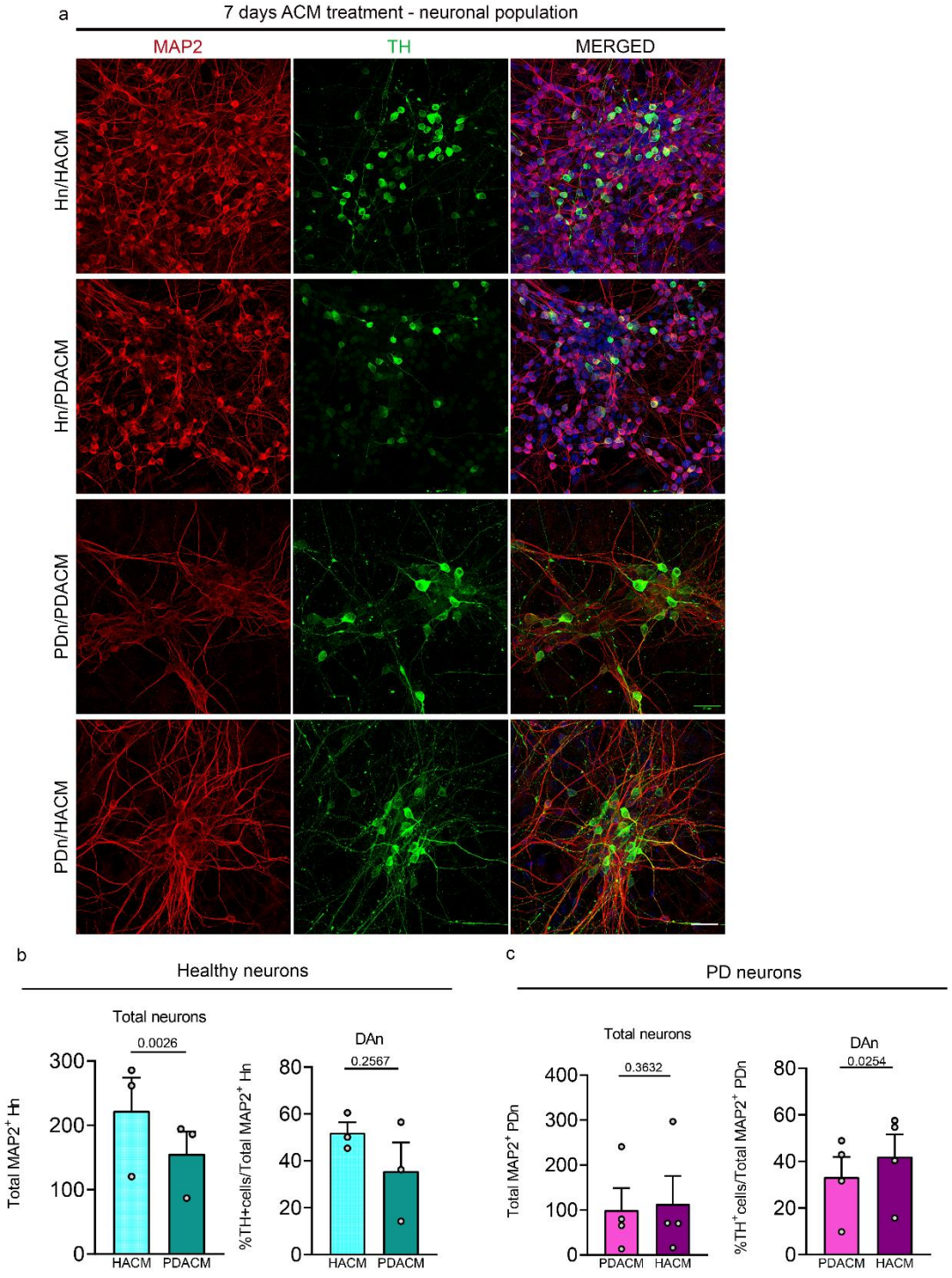


**Figure 11. Astrocyte conditioned media affect neuronal populations| a.** Representative confocal images of 7-d treated Hn with HACM or PDACM and PDn with HACM or PDACM, after immunostaining for MAP2 (red) and TH (green). Scale bar: 30 µm. **b.** Bar plots showing the quantification of total ($MAP2^+$) and DA ($TH^+$) Hn after HACM or PDACM treatment. **c.** Bar plots showing the quantification of total ($MAP2^+$) and DA ($TH^+$) PDn. Data are presented as mean ± SEM. Ratio-paired t-test was used for

comparisons. Sample sizes: n = 3 Hn and n = 4 PDn (including the isogenic pair) from separate experiments.

*HACM, Healthy Astrocyte-Conditioned Medium; PDACM, PD Astrocyte-Conditioned Medium; Ha, healthy astrocytes; Hn, healthy neurons; PDn, p.A53T-αSyn neurons; PDa, p.A53T-αSyn astrocytes; TH, tyrosine hydroxylase; MAP2, Microtubule-associated protein 2; SEM, standard error of the mean.*

## Healthy astrocyte-conditioned media improve neuronal network density of PD neurons

Co-culture of PDn with Ha improves neurite outgrowth and branching, compared to being co-cultured with PDa (Paschou, Apokotou et al., under submission). To address whether ACM affects neuronal network structure we treated PDn and Hn with conditioned medium from PDa and Ha at all possible combinations. After 1-week treatment with ACM, we assessed the density of $MAP2^+$ neuronal network by measuring the intensity of MAP2 thresholded area. We found that MAP2 area of Hn was slightly reduced (without reaching significance) after treatment with ACM from PDa, as compared to healthy conditioned medium treatment (Fig. 12a). Interestingly, PDn network density displayed a trend for improvement after treatment with ACM from Ha, as compared to PDACM (Fig. 12a), indicating a putative protective effect against pathological network formation. In line, we observed that Hn treated with ACM from PDa were organized in dense groups of cells "clumps" indicating increased stress levels (Kepiro et al., 2018). PDn treated with ACM from Ha tend to be organized more uniformly with less clumps compared to being treated with PDACM (Fig. 12b). Overall, it is indicated that the secretome of healthy astrocytes is able to improve pathological network of PD neurons and enhance normal neuronal growth. However, more biological replicates are necessary to empower those findings.

Title: Astrocyte Dysfunction in Parkinson's Disease: Insights from Neuron-Astrocyte Interactions in a Patient-Derived Model
Student Name: Sofia Dede

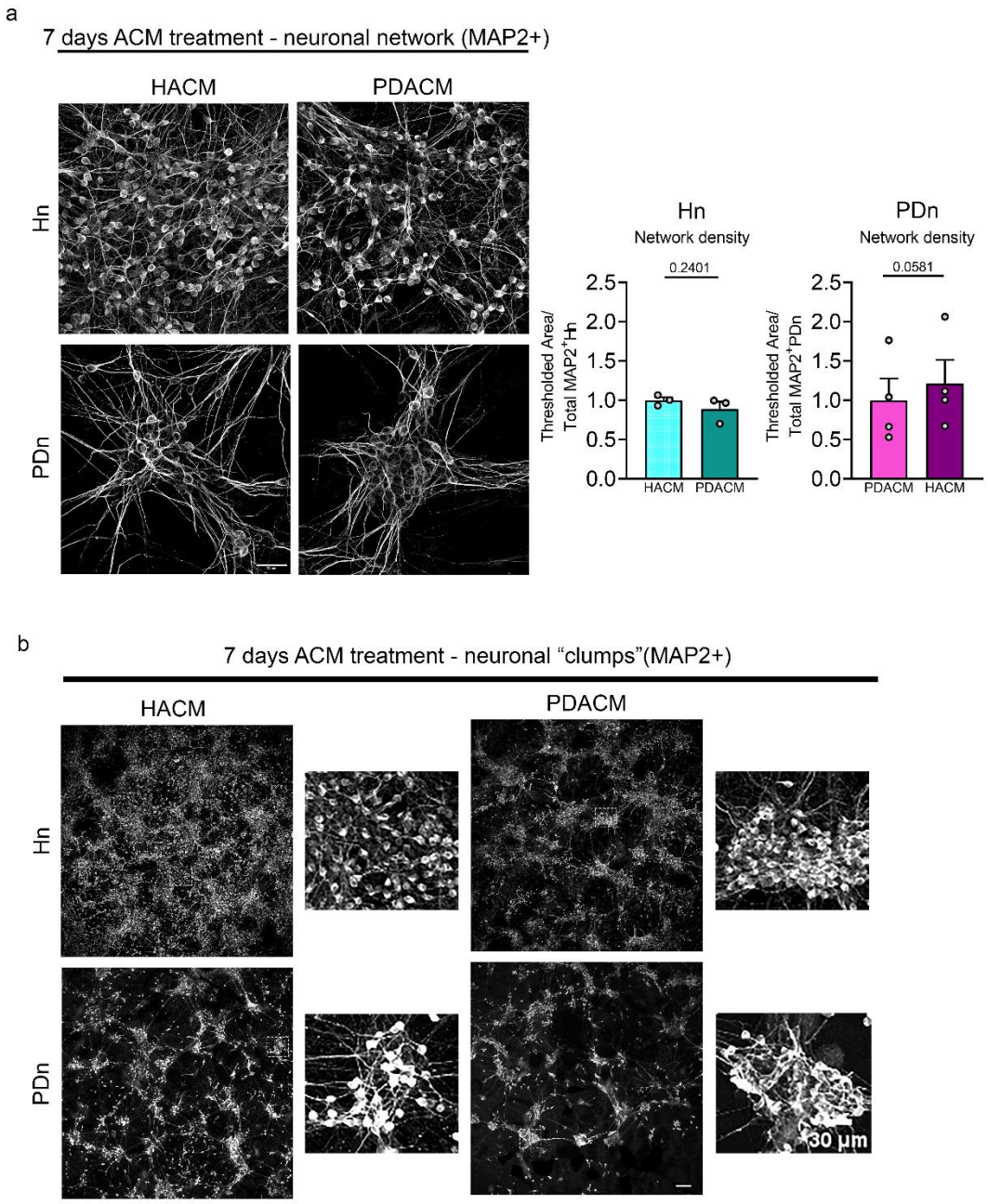


**Figure 12. Impact of ACM in neuronal network after a 7-d treatment| a.** Representative confocal images of 7-d treated Hn with HACM or PDACM and PDn with HACM or PDACM, after immunostaining for MAP2 (white). Scale bar: 30 µm. Accompanying bar plots showing the quantification of neuronal network ($MAP2^+$) density in Hn and PDn after HACM or PDACM. **b.** Representative confocal images of 7-d treated Hn with HACM or PDACM and PDn with HACM or PDACM, after immunostaining for MAP2 (white). Magnifications of the boxed areas with neuronal "clumps" are shown in insets. Scale bar: 100 µm. Scale bar, inset: 30 µm. Data are presented as mean ± SEM. Ratio-paired t-test was used for comparisons. Sample sizes: n = 3 Hn and n = 4 PDn (including the isogenic pair) from separate experiments.

*HACM, Healthy Astrocyte-Conditioned Medium; PDACM, PD Astrocyte-Conditioned Medium; Ha, healthy astrocytes; Hn, healthy neurons; PDn, p.A53T-αSyn neurons; PDa, p.A53T-αSyn astrocytes; MAP2, Microtubule-associated protein 2; SEM, standard error of the mean.*

## Discussion

Leveraging PD patient-derived iPSCs, this study demonstrates that the endogenous expression of mutant p.A53T-αSyn in astrocytes induces critical intrinsic defects in their ability to maintain neuronal fitness. Our data highlight a non-cell autonomous aspect of PD neuropathology emanating from astrocytes. Astrocytes harboring the p.A53T-αSyn mutation could not properly uptake and degrade αSyn aggregates. In line, their lysosomes manifested functional deficits related with abnormal acidification and enzymatic activity. In a co-culture setup of SH-SY5Y neuroblastoma cells loaded with αSyn-PFFs and iAstrocytes, PDa were unable to reduce the load of αSyn-PFFs in neuronal cells as opposed to co-cultures with Ha, where the load was significantly less. PDa-conditioned media proved less competent than Ha-conditioned media in supporting clearance of aggregated proteins, which results in accumulation of protein aggregates in PDn, jeopardizing neuronal survival and network formation.

Second to microglia, astrocytes are proficient scavengers of αSyn species released by neurons in the extracellular space, efficiently degrading αSyn (Braidy et al., 2013; Fellner et al., 2013; H.-J. Lee et al., 2010; Loria et al., 2017; Tsunemi et al., 2020). However, upon extensive αSyn internalization, overcharge of the endo-lysosomal pathway results to large intracellular deposits in astrocytes, suggesting incomplete digestion (Lindström et al., 2017b), indicative of impaired phagocytosis (Filippini et al., 2019). Here we show that astrocytes carrying the p.A53T-αSyn mutation uptake neuronal αSyn less efficiently when compared to Ha, upon treatment with PDnCM, revealing delayed internalization. This might indicate a dysregulation in receptor-mediated phagocytosis mechanisms. Possible receptor candidates are Toll-like receptors (TLRs), such as the TLR2 and TLR4, have been reported to mediate uptake of αSyn in astrocytes (Fellner et al., 2013; Kim et al., 2018; H.-J. Lee et al., 2010). Alternatively, clusterin, an extracellular chaperone protein, interacts with αSyn-fibrils

affecting their conformation and aggregation state and therefore regulate αSyn internalization in astrocytes (Filippini et al., 2021). Proteomic analysis from our group revealed down-regulation of AnnexinA2 (ANXA2) in PDa (Paschou, Apokotou et al., under submission). ANXA2 is a $Ca^{2+}$-regulated protein involved in the regulation of phagocytosis (Law et al., 2009), endosome stabilization (Scharf et al., 2012), autophagy (Moreau et al., 2015; Morozova et al., 2015), and astrocytic clearance of extracellular αSyn aggregates, while abolishment of its expression leads to reduced αSyn internalization in astrocytes (Streubel-Gallasch et al., 2021). Additionally, among the most down-regulated proteins in PDa, according to the proteomic analysis, was GULP1, required for efficient astrocytic phagocytosis(Morizawa et al., 2017).

In addition to secretion-uptake-based mechanisms, TNT-related mechanisms are involved in direct cell-to-cell contact-mediated spreading of αSyn among astrocytes, or neurons and astrocytes (Loria et al., 2017; Rostami et al., 2017a). When Ha were exposed to αSyn-PFFs, we noted a significantly increased TNT biogenesis, which is in agreement with previous publications (Raghavan et al., 2024; Rostami et al., 2017a). However, when PDa were exposed to αSyn-PFFs the induced TNT formation did not reach significance, indicating a pre-existing stress due to the p.A53T-αSyn mutation. In line, we report for the first time increased TNT biogenesis in PDa under normal and stress-induced conditions, when compared to Ha, suggesting a correlation between the p.A53T-αSyn mutation and enhanced TNT formation. It is supported that increased TNT generation is a stress-induced survival strategy in an attempt of the cell to "seek for help". A general theory suggests that αSyn-aggregate overload inside the cells leads to a cascade of reactions causing lysosomal stress, ROS production, and mitochondrial dysfunction, indicating that the formation of TNTs may be related to oxidative stress associated with accumulation of aggregates (Victoria & Zurzolo, 2017). A recent study proposed a mechanism whereby treatment of astrocytes with αSyn-fibrils leads to transient translocation of Focal Adhesion Kinase (FAK) to the nucleus, promoting TNT biogenesis to rescue cells from αSyn toxic burden (Raghavan et al., 2024). Disease is considered a TNT-inducing factor (Zhou et al., 2024). Here we showed that astrocytes harboring the p.A53T-αSyn mutation

exhibited enhanced TNT biogenesis, possibly caused by innate deficits, such as lysosomal disfunction. The use of cryo-electron tomography, electron microscopy, and most importantly, real-time imaging technology are necessary to establish the existence of fully functional TNTs in our iAstrocytes, and ensure αSyn transfer through TNTs. The assessment of neuron-to-astrocyte TNT-mediated transfer of αSyn-PFFs is ongoing and places a future objective.

Our observations (this study and unpublished data) largely share a common denominator; the dysregulation of the lysosomal function, converging with previous studies to suggest a major role of lysosomal disruption in PD pathogenesis (Klein & Mazzulli, 2018), but here in the less-acknowledged astrocytic component. In support, our data revealed a disturbance of lysosomal function in PDa that was reflected in the increased number of lysosomes, decreased lysosomal lumen acidity, and, ultimately, reduced Cathepsin B activity. In a recent study, iPSC-derived astrocytes from Gaucher disease (GD) patients exhibited reduced levels of Cathepsin D activity, leading to αSyn accumulation and inflammatory response (Aflaki et al., 2020). Further, our proteomic analysis revealed that mutant p.A53T-αSyn expression in PDa resulted in down-regulation of ATP6V0D1, subunit d1 of V-type $H^+$-ATPase in the integral membrane V0 complex, responsible for acidifying intracellular compartments including the lysosomes(L. Wang et al., 2020). Additionally, lysosomal enzyme galactosylceraminidase (GALC) expression was found up-regulated in PDa. GALC is involved in glycosphingolipid degradation with pathogenic gene variants linked with Krabbe disease, an infantile neurodegenerative lysosomal storage disorder. Further, up-regulation was detected in RAB12, a Ras-related small GTPase found in vesicular compartments related to endosome function with critical involvement in PD (Steger et al., 2016), reported as regulator of LRRK2 activity in response to lysosomal damage(X. Wang et al., 2023). Finally, previous studies have shown that when astrocytic degradation potential is limited due to extensive uptake of αSyn aggregates or a hereditary PD-related mutation, this inevitably leads to impaired capability of astrocytes to support neuronal metabolism and synaptic function (Lindström et al., 2017a; Tsunemi et al., 2020). Those studies are in agreement with our findings indicating that p.A53T-αSyn mutation in astrocytes leads to

dysfunctional lysosomal clearance of exogenously added αSyn-PFFs and αSyn accumulation, which explains PDa inability to rescue SH-SY5Y neuronal cells from αSyn-load in co-culture.

Astrocytes are crucial players for the protection and maintenance of neuronal survival and healthy neuronal network, mediating the release of neurotrophic factors and anti-inflammatory cytokines (Cabezas et al., 2014; Du et al., 2018). Our results indicate that Ha partially restore neuronal survival, especially that of dopaminergic neurons, and network formation of PDn by paracrine mediators. In line, media conditioned by healthy astrocytes rescued cell survival and morphological alterations of iPSC-derived dopaminergic neurons from PD patients with LRRK2 G2019S mutation (di Domenico et al., 2019). Conversely, when Hn were treated with media conditioned by PDa, we detected a decrease in dopaminergic and total neuronal populations. Supporting our findings, decreased dopaminergic neuronal survival caused by factors secreted by PDa has been reported, indicating a neurotoxic potential of PDa at least partially mediated by their secretome (di Domenico et al., 2019; Pons-Espinal et al., 2024; Qiao et al., 2016). Importantly, medium conditioned by Ha was able to decrease the levels of protein aggregates and αSyn containing aggregates in PDn, indicating that direct neuron-astrocyte contact is not necessary for the astrocytic neuroprotective function. ACM-mediated reduction of misfolded αSyn aggregates in neurons was highlighted previously (di Domenico et al., 2019; Yang et al., 2022). Further, Yang et.al 2022 showed inhibition of intraneuronal αSyn oligomerization, promotion of extracellular αSyn aggregates disassembly and stimulation of neuronal autophagic clearance of αSyn, all mediated by conditioned media from healthy astrocytes, in a paracrine manner. The factors that are secreted by astrocytes and facilitate the observed anti-synucleinopathic functions remain to be further defined. Protein disulfide isomerase (PDI) a chaperone and oxidoreductase, with the capacity to dissolve or prevent the aggregation of αSyn has been detected as a component of ACM (Serrano et al., 2020; Yang et al., 2022). Interferon-β (IFNβ) is another candidate molecule with paracrine action, reported to be highly expressed/secreted by cultured astrocytes and to promote autophagic flux and αSyn degradation in neurons (Ejlerskov et al., 2015; Song et al., 2017). Further

molecules and underling mechanisms of astrocytic paracrine effects in neurons need to be addressed in the future.

In conclusion, the p.A53T-αSyn mutation drives astrocytic pathology, leads to malfunction of cellular clearance mechanisms and alters normal astrocytic secretome composition, rendering PD astrocytes incompetent to rescue neurons from αSyn-load and support neuronal fitness. Further, it is demonstrated that healthy astrocytes secrete factors facilitating anti-synucleinopathic functions, reducing neuronal αSyn aggregates and offering neuroprotection. The identification of these molecules is of high importance and may be utilized for the development of potential PD treatment. Finally, the p.A53T-αSyn mutation leads to increased TNT-biogenesis in astrocytes, as a possible contact-mediated mechanism for αSyn transfer, providing the ground for further research to elucidate the underling mechanisms.

## Acknowledgments

This research thesis would not have been possible without the guidance and support of many individuals. First and foremost, I would like to express my deepest gratitude to my supervisor, Dr. Florentia Papastefanaki, for her constant support, guidance, and encouragement throughout this journey. Her insightful feedback and patience were invaluable in shaping my thesis and helping me overcome numerous challenges along the way. I am extremely fortunate to have had the opportunity to work under her mentorship. I am also deeply thankful to Dr. Rebecca Matsas for her valuable insights and constructive feedback, which greatly enriched my research project. I would further like to express my sincere gratitude to Prof. Chiara Zurzolo, director of the Laboratory of Membrane Traffic and Pathogenesis, for giving me the opportunity to conduct a part of my master's thesis research in her lab at Institut Pasteur in Paris. I would also like to thank Dr. Era Taoufik for her support and for generously sharing her knowledge and expertise. Additionally, I would like to thank my colleagues at Hellenic Pasteur Institute and Institut Pasteur Paris for providing a collaborative and positive environment. I am especially grateful to my Stem-cell lab partners Olympia Apokotou, Christina Paschou, Anastasios Kollias and Evanthia Tselo for their constant

encouragement, guidance and companionship. Further, I would like to give special thanks to my lab partners in Paris, Francesca Palese and Ranabir Chakraborty, for their continuous support and insightful discussions. My sincere thanks also go to Katerina Segklia and Sevan Belian for their practical advice and for always being available to answer my questions. Lastly, I wish to thank my family and friends for their unending patience and encouragement.

Supported by the Hellenic Foundation for Research and Innovation (H.F.R.I.) under the "1st Call for H.F.R.I. Research Projects to support Faculty members and Researchers and the procurement of high-cost research equipment" (Project 1019-DiseasePhenoTarget). Funded by PIU – Pasteur International Unit between the Hellenic Pasteur Institute and Institut Pasteur Paris "Creation of a Virtual Research Unit for Studies in Neurodegenerative Diseases". Supported by Bodossaki Foundation (Scholarship Programme for Visiting Research Scientists) and Federation of European Neuroscience Societies (FENS/IBRO-PERC Exchange Fellowships Programme).

## No plagiarism statement

The Authors confirm that intact sentences or paragraphs from other publications are not included and that there is no significant overlap with other publications

## Bibliography

1. Abounit, S., Bousset, L., Loria, F., Zhu, S., de Chaumont, F., Pieri, L., Olivo-Marin, J., Melki, R., & Zurzolo, C. (2016). Tunneling nanotubes spread fibrillar α-synuclein by intercellular trafficking of lysosomes. *The EMBO Journal*, *35*(19), 2120–2138. https://doi.org/10.15252/embj.201593411
2. Abounit, S., & Zurzolo, C. (2012). Wiring through tunneling nanotubes – from electrical signals to organelle transfer. *Journal of Cell Science*, *125*(5), 1089–1098. https://doi.org/10.1242/jcs.083279
3. Aflaki, E., Stubblefield, B. K., McGlinchey, R. P., McMahon, B., Ory, D. S., & Sidransky, E. (2020). A characterization of Gaucher iPS-derived astrocytes: Potential implications for Parkinson's disease. *Neurobiology of Disease*, *134*, 104647. https://doi.org/10.1016/j.nbd.2019.104647
4. Altay, M. F., Liu, A. K. L., Holton, J. L., Parkkinen, L., & Lashuel, H. A. (2022). Prominent astrocytic alpha-synuclein pathology with unique post-translational

modification signatures unveiled across Lewy body disorders. *Acta Neuropathologica Communications*, *10*(1), 163. https://doi.org/10.1186/s40478-022-01468-8

5. Antoniou, N., Prodromidou, K., Kouroupi, G., Boumpoureka, I., Samiotaki, M., Panayotou, G., Xilouri, M., Kloukina, I., Stefanis, L., Grailhe, R., Taoufik, E., & Matsas, R. (2022). High content screening and proteomic analysis identify a kinase inhibitor that rescues pathological phenotypes in a patient-derived model of Parkinson's disease. *Npj Parkinson's Disease*, *8*(1), 15. https://doi.org/10.1038/s41531-022-00278-y
6. Barbar, L., Jain, T., Zimmer, M., Kruglikov, I., Sadick, J. S., Wang, M., Kalpana, K., Rose, I. V. L., Burstein, S. R., Rusielewicz, T., Nijsure, M., Guttenplan, K. A., di Domenico, A., Croft, G., Zhang, B., Nobuta, H., Hébert, J. M., Liddelow, S. A., & Fossati, V. (2020). CD49f Is a Novel Marker of Functional and Reactive Human iPSC-Derived Astrocytes. *Neuron*, *107*(3), 436-453.e12. https://doi.org/10.1016/j.neuron.2020.05.014
7. Barbar, L., Rusielewicz, T., Zimmer, M., Kalpana, K., & Fossati, V. (2020). Isolation of Human CD49f+ Astrocytes and In Vitro iPSC-Based Neurotoxicity Assays. *STAR Protocols*, *1*(3), 100172. https://doi.org/10.1016/j.xpro.2020.100172
8. Bendor, J. T., Logan, T. P., & Edwards, R. H. (2013). The Function of α-Synuclein. *Neuron*, *79*(6), 1044–1066. https://doi.org/10.1016/j.neuron.2013.09.004
9. Bloem, B. R., Okun, M. S., & Klein, C. (2021). Parkinson's disease. *The Lancet*, *397*(10291), 2284–2303. https://doi.org/10.1016/S0140-6736(21)00218-X
10. Booth, H. D. E., Hirst, W. D., & Wade-Martins, R. (2017). The Role of Astrocyte Dysfunction in Parkinson's Disease Pathogenesis. *Trends in Neurosciences*, *40*(6), 358–370. https://doi.org/10.1016/j.tins.2017.04.001
11. Braak, H., Sandmann-Keil, D., Gai, W., & Braak, E. (1999). Extensive axonal Lewy neurites in Parkinson's disease: a novel pathological feature revealed by α-synuclein immunocytochemistry. *Neuroscience Letters*, *265*(1), 67–69. https://doi.org/10.1016/S0304-3940(99)00208-6
12. Braak, H., Sastre, M., & Del Tredici, K. (2007). Development of α-synuclein immunoreactive astrocytes in the forebrain parallels stages of intraneuronal pathology in sporadic Parkinson's disease. *Acta Neuropathologica*, *114*(3), 231–241. https://doi.org/10.1007/s00401-007-0244-3
13. Braidy, N., Gai, W.-P., Xu, Y. H., Sachdev, P., Guillemin, G. J., Jiang, X.-M., Ballard, J. W. O., Horan, M. P., Fang, Z. M., Chong, B. H., & Chan, D. Y. (2013). Uptake and mitochondrial dysfunction of alpha-synuclein in human astrocytes, cortical neurons and fibroblasts. *Translational Neurodegeneration*, *2*(1), 20. https://doi.org/10.1186/2047-9158-2-20
14. Brandebura, A. N., Paumier, A., Onur, T. S., & Allen, N. J. (2023). Astrocyte contribution to dysfunction, risk and progression in neurodegenerative disorders. *Nature Reviews Neuroscience*, *24*(1), 23–39. https://doi.org/10.1038/s41583-022-00641-1
15. Breger, L. S., & Fuzzati Armentero, M. T. (2019). Genetically engineered animal models of Parkinson's disease: From worm to rodent. *European Journal of Neuroscience*, *49*(4), 533–560. https://doi.org/10.1111/ejn.14300
16. Cabezas, R., Ã□vila, M., Gonzalez, J., El-BachÃ¡, R. S., BÃ¡ez, E., GarcÃa-Segura, L. M., Jurado Coronel, J. C., Capani, F., Cardona-Gomez, G. P., & Barreto, G. E. (2014). Astrocytic modulation of blood brain barrier: perspectives on Parkinsonâ€TMs

disease. *Frontiers in Cellular Neuroscience*, *8*. https://doi.org/10.3389/fncel.2014.00211

17. Chakraborty, R., Nonaka, T., Hasegawa, M., & Zurzolo, C. (2023). Tunnelling nanotubes between neuronal and microglial cells allow bi-directional transfer of α-Synuclein and mitochondria. *Cell Death & Disease*, *14*(5), 329. https://doi.org/10.1038/s41419-023-05835-8
18. De Luca, C., Colangelo, A. M., Alberghina, L., & Papa, M. (2018). Neuro-Immune Hemostasis: Homeostasis and Diseases in the Central Nervous System. *Frontiers in Cellular Neuroscience*, *12*. https://doi.org/10.3389/fncel.2018.00459
19. de Rus Jacquet, A. (2019). Preparation and Co-Culture of iPSC-Derived Dopaminergic Neurons and Astrocytes. *Current Protocols in Cell Biology*, *85*(1). https://doi.org/10.1002/cpcb.98
20. Deng, H., Wang, P., & Jankovic, J. (2018). The genetics of Parkinson disease. *Ageing Research Reviews*, *42*, 72–85. https://doi.org/10.1016/j.arr.2017.12.007
21. di Domenico, A., Carola, G., Calatayud, C., Pons-Espinal, M., Muñoz, J. P., Richaud-Patin, Y., Fernandez-Carasa, I., Gut, M., Faella, A., Parameswaran, J., Soriano, J., Ferrer, I., Tolosa, E., Zorzano, A., Cuervo, A. M., Raya, A., & Consiglio, A. (2019). Patient-Specific iPSC-Derived Astrocytes Contribute to Non-Cell-Autonomous Neurodegeneration in Parkinson's Disease. *Stem Cell Reports*, *12*(2), 213–229. https://doi.org/10.1016/j.stemcr.2018.12.011
22. Dilsizoglu Senol, A., Samarani, M., Syan, S., Guardia, C. M., Nonaka, T., Liv, N., Latour-Lambert, P., Hasegawa, M., Klumperman, J., Bonifacino, J. S., & Zurzolo, C. (2021). α-Synuclein fibrils subvert lysosome structure and function for the propagation of protein misfolding between cells through tunneling nanotubes. *PLOS Biology*, *19*(7), e3001287. https://doi.org/10.1371/journal.pbio.3001287
23. Du, F., Yu, Q., Chen, A., Chen, D., & Yan, S. S. (2018). Astrocytes Attenuate Mitochondrial Dysfunctions in Human Dopaminergic Neurons Derived from iPSC. *Stem Cell Reports*, *10*(2), 366–374. https://doi.org/10.1016/j.stemcr.2017.12.021
24. Ejlerskov, P., Hultberg, J. G., Wang, J., Carlsson, R., Ambjørn, M., Kuss, M., Liu, Y., Porcu, G., Kolkova, K., Friis Rundsten, C., Ruscher, K., Pakkenberg, B., Goldmann, T., Loreth, D., Prinz, M., Rubinsztein, D. C., & Issazadeh-Navikas, S. (2015). Lack of Neuronal IFN-β-IFNAR Causes Lewy Body- and Parkinson's Disease-like Dementia. *Cell*, *163*(2), 324–339. https://doi.org/10.1016/j.cell.2015.08.069
25. Emmanouilidou, E., Melachroinou, K., Roumeliotis, T., Garbis, S. D., Ntzouni, M., Margaritis, L. H., Stefanis, L., & Vekrellis, K. (2010a). Cell-Produced α-Synuclein Is Secreted in a Calcium-Dependent Manner by Exosomes and Impacts Neuronal Survival. *The Journal of Neuroscience*, *30*(20), 6838–6851. https://doi.org/10.1523/JNEUROSCI.5699-09.2010
26. Fellner, L., Irschick, R., Schanda, K., Reindl, M., Klimaschewski, L., Poewe, W., Wenning, G. K., & Stefanova, N. (2013). Toll-like receptor 4 is required for α-synuclein dependent activation of microglia and astroglia. *Glia*, *61*(3), 349–360. https://doi.org/10.1002/glia.22437
27. Filippini, A., Gennarelli, M., & Russo, I. (2019). α-Synuclein and Glia in Parkinson's Disease: A Beneficial or a Detrimental Duet for the Endo-Lysosomal System? *Cellular and Molecular Neurobiology*, *39*(2), 161–168. https://doi.org/10.1007/s10571-019-00649-9

28. Filippini, A., Mutti, V., Faustini, G., Longhena, F., Ramazzina, I., Rizzi, F., Kaganovich, A., Roosen, D. A., Landeck, N., Duffy, M., Tessari, I., Bono, F., Fiorentini, C., Greggio, E., Bubacco, L., Bellucci, A., Missale, M., Cookson, M. R., Gennarelli, M., & Russo, I. (2021). Extracellular clusterin limits the uptake of α-synuclein fibrils by murine and human astrocytes. *Glia*, *69*(3), 681–696. https://doi.org/10.1002/glia.23920
29. Grigor'eva, E. V., Kopytova, A. E., Yarkova, E. S., Pavlova, S. V., Sorogina, D. A., Malakhova, A. A., Malankhanova, T. B., Baydakova, G. V., Zakharova, E. Y., Medvedev, S. P., Pchelina, S. N., & Zakian, S. M. (2023). Biochemical Characteristics of iPSC-Derived Dopaminergic Neurons from N370S GBA Variant Carriers with and without Parkinson's Disease. *International Journal of Molecular Sciences*, *24*(5), 4437. https://doi.org/10.3390/ijms24054437
30. Henry, A. G., Aghamohammadzadeh, S., Samaroo, H., Chen, Y., Mou, K., Needle, E., & Hirst, W. D. (2015). Pathogenic LRRK2 mutations, through increased kinase activity, produce enlarged lysosomes with reduced degradative capacity and increase ATP13A2 expression. *Human Molecular Genetics*, *24*(21), 6013–6028. https://doi.org/10.1093/hmg/ddv314
31. Kepiro, M., Varkuti, B. H., & Davis, R. L. (2018). *High Content, Phenotypic Assays and Screens for Compounds Modulating Cellular Processes in Primary Neurons* (pp. 219–250). https://doi.org/10.1016/bs.mie.2018.09.021
32. Kim, C., Spencer, B., Rockenstein, E., Yamakado, H., Mante, M., Adame, A., Fields, J. A., Masliah, D., Iba, M., Lee, H.-J., Rissman, R. A., Lee, S.-J., & Masliah, E. (2018). Immunotherapy targeting toll-like receptor 2 alleviates neurodegeneration in models of synucleinopathy by modulating α-synuclein transmission and neuroinflammation. *Molecular Neurodegeneration*, *13*(1), 43. https://doi.org/10.1186/s13024-018-0276-2
33. Klein, A. D., & Mazzulli, J. R. (2018). Is Parkinson's disease a lysosomal disorder? *Brain*, *141*(8), 2255–2262. https://doi.org/10.1093/brain/awy147
34. Kostuk, E. W., Cai, J., & Iacovitti, L. (2019). Subregional differences in astrocytes underlie selective neurodegeneration or protection in Parkinson's disease models in culture. *Glia*, *67*(8), 1542–1557. https://doi.org/10.1002/glia.23627
35. Kouroupi, G., Taoufik, E., Vlachos, I. S., Tsioras, K., Antoniou, N., Papastefanaki, F., Chroni-Tzartou, D., Wrasidlo, W., Bohl, D., Stellas, D., Politis, P. K., Vekrellis, K., Papadimitriou, D., Stefanis, L., Bregestovski, P., Hatzigeorgiou, A. G., Masliah, E., & Matsas, R. (2017). Defective synaptic connectivity and axonal neuropathology in a human iPSC-based model of familial Parkinson's disease. *Proceedings of the National Academy of Sciences*, *114*(18). https://doi.org/10.1073/pnas.1617259114
36. Kriks, S., Shim, J.-W., Piao, J., Ganat, Y. M., Wakeman, D. R., Xie, Z., Carrillo-Reid, L., Auyeung, G., Antonacci, C., Buch, A., Yang, L., Beal, M. F., Surmeier, D. J., Kordower, J. H., Tabar, V., & Studer, L. (2011). Dopamine neurons derived from human ES cells efficiently engraft in animal models of Parkinson's disease. *Nature*, *480*(7378), 547–551. https://doi.org/10.1038/nature10648
37. Lashuel, H. A., Overk, C. R., Oueslati, A., & Masliah, E. (2013a). The many faces of α-synuclein: from structure and toxicity to therapeutic target. *Nature Reviews Neuroscience*, *14*(1), 38–48. https://doi.org/10.1038/nrn3406
38. Lashuel, H. A., Overk, C. R., Oueslati, A., & Masliah, E. (2013b). The many faces of α-synuclein: from structure and toxicity to therapeutic target. *Nature Reviews Neuroscience*, *14*(1), 38–48. https://doi.org/10.1038/nrn3406

39. Law, A.-L., Ling, Q., Hajjar, K. A., Futter, C. E., Greenwood, J., Adamson, P., Wavre-Shapton, S. T., Moss, S. E., & Hayes, M. J. (2009). Annexin A2 Regulates Phagocytosis of Photoreceptor Outer Segments in the Mouse Retina. *Molecular Biology of the Cell*, *20*(17), 3896–3904. https://doi.org/10.1091/mbc.e08-12-1204
40. Lázaro, D. F., Pavlou, M. A. S., & Outeiro, T. F. (2017). Cellular models as tools for the study of the role of alpha-synuclein in Parkinson's disease. *Experimental Neurology*, *298*, 162–171. https://doi.org/10.1016/j.expneurol.2017.05.007
41. Lee, H.-J., Suk, J.-E., Patrick, C., Bae, E.-J., Cho, J.-H., Rho, S., Hwang, D., Masliah, E., & Lee, S.-J. (2010). Direct Transfer of α-Synuclein from Neuron to Astroglia Causes Inflammatory Responses in Synucleinopathies. *Journal of Biological Chemistry*, *285*(12), 9262–9272. https://doi.org/10.1074/jbc.M109.081125
42. Lee, S.-I., Jeong, W., Lim, H., Cho, S., Lee, H., Jang, Y., Cho, J., Bae, S., Lin, Y.-T., Tsai, L.-H., Moon, D. W., & Seo, J. (2021). APOE4-carrying human astrocytes oversupply cholesterol to promote neuronal lipid raft expansion and Aβ generation. *Stem Cell Reports*, *16*(9), 2128–2137. https://doi.org/10.1016/j.stemcr.2021.07.017
43. Liddelow, S. A., & Barres, B. A. (2017). Reactive Astrocytes: Production, Function, and Therapeutic Potential. *Immunity*, *46*(6), 957–967. https://doi.org/10.1016/j.immuni.2017.06.006
44. Lindström, V., Gustafsson, G., Sanders, L. H., Howlett, E. H., Sigvardson, J., Kasrayan, A., Ingelsson, M., Bergström, J., & Erlandsson, A. (2017a). Extensive uptake of α-synuclein oligomers in astrocytes results in sustained intracellular deposits and mitochondrial damage. *Molecular and Cellular Neuroscience*, *82*, 143–156. https://doi.org/10.1016/j.mcn.2017.04.009
45. Livak, K. J., & Schmittgen, T. D. (2001). Analysis of Relative Gene Expression Data Using Real-Time Quantitative PCR and the 2−ΔΔCT Method. *Methods*, *25*(4), 402–408. https://doi.org/10.1006/meth.2001.1262
46. Lo, C. H., & Zeng, J. (2023). Defective lysosomal acidification: a new prognostic marker and therapeutic target for neurodegenerative diseases. *Translational Neurodegeneration*, *12*(1), 29. https://doi.org/10.1186/s40035-023-00362-0
47. Loria, F., Vargas, J. Y., Bousset, L., Syan, S., Salles, A., Melki, R., & Zurzolo, C. (2017). α-Synuclein transfer between neurons and astrocytes indicates that astrocytes play a role in degradation rather than in spreading. *Acta Neuropathologica*, *134*(5), 789–808. https://doi.org/10.1007/s00401-017-1746-2
48. Ludwig, T. E., Andrews, P. W., Barbaric, I., Benvenisty, N., Bhattacharyya, A., Crook, J. M., Daheron, L. M., Draper, J. S., Healy, L. E., Huch, M., Inamdar, M. S., Jensen, K. B., Kurtz, A., Lancaster, M. A., Liberali, P., Lutolf, M. P., Mummery, C. L., Pera, M. F., Sato, Y., … Mosher, J. T. (2023). ISSCR standards for the use of human stem cells in basic research. *Stem Cell Reports*, *18*(9), 1744–1752. https://doi.org/10.1016/j.stemcr.2023.08.003
49. Luk, K. C., Song, C., O'Brien, P., Stieber, A., Branch, J. R., Brunden, K. R., Trojanowski, J. Q., & Lee, V. M.-Y. (2009). Exogenous α-synuclein fibrils seed the formation of Lewy body-like intracellular inclusions in cultured cells. *Proceedings of the National Academy of Sciences*, *106*(47), 20051–20056. https://doi.org/10.1073/pnas.0908005106
50. Masaracchia, C., Hnida, M., Gerhardt, E., Lopes da Fonseca, T., Villar-Pique, A., Branco, T., Stahlberg, M. A., Dean, C., Fernández, C. O., Milosevic, I., & Outeiro, T. F. (2018). Membrane binding, internalization, and sorting of alpha-synuclein in the cell.

*Acta Neuropathologica Communications*, *6*(1), 79. https://doi.org/10.1186/s40478-018-0578-1

51. Meng, Y., Ding, J., Li, C., Fan, H., He, Y., & Qiu, P. (2020). Transfer of pathological α-synuclein from neurons to astrocytes via exosomes causes inflammatory responses after METH exposure. *Toxicology Letters*, *331*, 188–199. https://doi.org/10.1016/j.toxlet.2020.06.016
52. Miller, S. J. (2018). Astrocyte Heterogeneity in the Adult Central Nervous System. *Frontiers in Cellular Neuroscience*, *12*. https://doi.org/10.3389/fncel.2018.00401
53. Moreau, K., Ghislat, G., Hochfeld, W., Renna, M., Zavodszky, E., Runwal, G., Puri, C., Lee, S., Siddiqi, F., Menzies, F. M., Ravikumar, B., & Rubinsztein, D. C. (2015). Transcriptional regulation of Annexin A2 promotes starvation-induced autophagy. *Nature Communications*, *6*(1), 8045. https://doi.org/10.1038/ncomms9045
54. Morizawa, Y. M., Hirayama, Y., Ohno, N., Shibata, S., Shigetomi, E., Sui, Y., Nabekura, J., Sato, K., Okajima, F., Takebayashi, H., Okano, H., & Koizumi, S. (2017). Reactive astrocytes function as phagocytes after brain ischemia via ABCA1-mediated pathway. *Nature Communications*, *8*(1), 28. https://doi.org/10.1038/s41467-017-00037-1
55. Morozova, K., Sidhar, S., Zolla, V., Clement, C. C., Scharf, B., Verzani, Z., Diaz, A., Larocca, J. N., Hajjar, K. A., Cuervo, A. M., & Santambrogio, L. (2015). Annexin A2 promotes phagophore assembly by enhancing Atg16L+ vesicle biogenesis and homotypic fusion. *Nature Communications*, *6*(1), 5856. https://doi.org/10.1038/ncomms6856
56. Mutvei, A. P., Nagiec, M. J., & Blenis, J. (2023). Balancing lysosome abundance in health and disease. *Nature Cell Biology*, *25*(9), 1254–1264. https://doi.org/10.1038/s41556-023-01197-7
57. Nonaka, T., Watanabe, S. T., Iwatsubo, T., & Hasegawa, M. (2010). Seeded Aggregation and Toxicity of α-Synuclein and Tau. *Journal of Biological Chemistry*, *285*(45), 34885–34898. https://doi.org/10.1074/jbc.M110.148460
58. Poewe, W., Seppi, K., Tanner, C. M., Halliday, G. M., Brundin, P., Volkmann, J., Schrag, A.-E., & Lang, A. E. (2017). Parkinson disease. *Nature Reviews Disease Primers*, *3*(1), 17013. https://doi.org/10.1038/nrdp.2017.13
59. Polymeropoulos, M. H., Lavedan, C., Leroy, E., Ide, S. E., Dehejia, A., Dutra, A., Pike, B., Root, H., Rubenstein, J., Boyer, R., Stenroos, E. S., Chandrasekharappa, S., Athanassiadou, A., Papapetropoulos, T., Johnson, W. G., Lazzarini, A. M., Duvoisin, R. C., Di Iorio, G., Golbe, L. I., & Nussbaum, R. L. (1997). Mutation in the α-Synuclein Gene Identified in Families with Parkinson's Disease. *Science*, *276*(5321), 2045–2047. https://doi.org/10.1126/science.276.5321.2045
60. Pons-Espinal, M., Blasco-Agell, L., Fernandez-Carasa, I., Andrés-Benito, P., di Domenico, A., Richaud-Patin, Y., Baruffi, V., Marruecos, L., Espinosa, L., Garrido, A., Tolosa, E., Edel, M. J., Otero, M. J., Mosquera, J. L., Ferrer, I., Raya, A., & Consiglio, A. (2024). Blocking IL-6 signaling prevents astrocyte-induced neurodegeneration in an iPSC-based model of Parkinson's disease. *JCI Insight*, *9*(3). https://doi.org/10.1172/jci.insight.163359
61. Puschmann, A. (2017). New Genes Causing Hereditary Parkinson's Disease or Parkinsonism. *Current Neurology and Neuroscience Reports*, *17*(9), 66. https://doi.org/10.1007/s11910-017-0780-8

62. Qiao, C., Yin, N., Gu, H., Zhu, J., Ding, J., Lu, M., & Hu, G. (2016). *Atp13a2* Deficiency Aggravates Astrocyte-Mediated Neuroinflammation via <scp>NLRP</scp> 3 Inflammasome Activation. *CNS Neuroscience & Therapeutics*, *22*(6), 451–460. https://doi.org/10.1111/cns.12514
63. Raghavan, A., Kashyap, R., Sreedevi, P., Jos, S., Chatterjee, S., Alex, A., D'Souza, M. N., Giridharan, M., Muddashetty, R., Manjithaya, R., Padavattan, S., & Nath, S. (2024). Astroglia proliferate upon the biogenesis of tunneling nanotubes via α-synuclein dependent transient nuclear translocation of focal adhesion kinase. *IScience*, *27*(8), 110565. https://doi.org/10.1016/j.isci.2024.110565
64. Rostami, J., Fotaki, G., Sirois, J., Mzezewa, R., Bergström, J., Essand, M., Healy, L., & Erlandsson, A. (2020). Astrocytes have the capacity to act as antigen-presenting cells in the Parkinson's disease brain. *Journal of Neuroinflammation*, *17*(1), 119. https://doi.org/10.1186/s12974-020-01776-7
65. Rostami, J., Holmqvist, S., Lindström, V., Sigvardson, J., Westermark, G. T., Ingelsson, M., Bergström, J., Roybon, L., & Erlandsson, A. (2017a). Human Astrocytes Transfer Aggregated Alpha-Synuclein via Tunneling Nanotubes. *The Journal of Neuroscience*, *37*(49), 11835–11853. https://doi.org/10.1523/JNEUROSCI.0983-17.2017
66. Rustom, A., Saffrich, R., Markovic, I., Walther, P., & Gerdes, H.-H. (2004). Nanotubular Highways for Intercellular Organelle Transport. *Science*, *303*(5660), 1007–1010. https://doi.org/10.1126/science.1093133
67. Schapira, A. H. V., & Tolosa, E. (2010). Molecular and clinical prodrome of Parkinson disease: implications for treatment. *Nature Reviews Neurology*, *6*(6), 309–317. https://doi.org/10.1038/nrneurol.2010.52
68. Scharf, B., Clement, C. C., Wu, X.-X., Morozova, K., Zanolini, D., Follenzi, A., Larocca, J. N., Levon, K., Sutterwala, F. S., Rand, J., Cobelli, N., Purdue, E., Hajjar, K. A., & Santambrogio, L. (2012). Annexin A2 binds to endosomes following organelle destabilization by particulate wear debris. *Nature Communications*, *3*(1), 755. https://doi.org/10.1038/ncomms1754
69. Schindelin, J., Arganda-Carreras, I., Frise, E., Kaynig, V., Longair, M., Pietzsch, T., Preibisch, S., Rueden, C., Saalfeld, S., Schmid, B., Tinevez, J.-Y., White, D. J., Hartenstein, V., Eliceiri, K., Tomancak, P., & Cardona, A. (2012). Fiji: an open-source platform for biological-image analysis. *Nature Methods*, *9*(7), 676–682. https://doi.org/10.1038/nmeth.2019
70. Serrano, A., Qiao, X., Matos, J. O., Farley, L., Cilenti, L., Chen, B., Tatulian, S. A., & Teter, K. (2020). Reversal of Alpha-Synuclein Fibrillization by Protein Disulfide Isomerase. *Frontiers in Cell and Developmental Biology*, *8*. https://doi.org/10.3389/fcell.2020.00726
71. Sharma, S. Das, Reddy, B. K., Pal, R., Ritakari, T. E., Cooper, J. D., Selvaraj, B. T., Kind, P. C., Chandran, S., Wyllie, D. J. A., & Chattarji, S. (2023). Astrocytes mediate cell non-autonomous correction of aberrant firing in human FXS neurons. *Cell Reports*, *42*(4), 112344. https://doi.org/10.1016/j.celrep.2023.112344
72. Sloan, S. A., & Barres, B. A. (2014). Mechanisms of astrocyte development and their contributions to neurodevelopmental disorders. *Current Opinion in Neurobiology*, *27*, 75–81. https://doi.org/10.1016/j.conb.2014.03.005
73. Sofroniew, M. V. (2009). Molecular dissection of reactive astrogliosis and glial scar formation. *Trends in Neurosciences*, *32*(12), 638–647. https://doi.org/10.1016/j.tins.2009.08.002

74. Soldner, F., Laganière, J., Cheng, A. W., Hockemeyer, D., Gao, Q., Alagappan, R., Khurana, V., Golbe, L. I., Myers, R. H., Lindquist, S., Zhang, L., Guschin, D., Fong, L. K., Vu, B. J., Meng, X., Urnov, F. D., Rebar, E. J., Gregory, P. D., Zhang, H. S., & Jaenisch, R. (2011). Generation of Isogenic Pluripotent Stem Cells Differing Exclusively at Two Early Onset Parkinson Point Mutations. *Cell*, *146*(2), 318–331. https://doi.org/10.1016/j.cell.2011.06.019
75. Song, J.-J., Oh, S.-M., Kwon, O.-C., Wulansari, N., Lee, H.-S., Chang, M.-Y., Lee, E., Sun, W., Lee, S.-E., Chang, S., An, H., Lee, C. J., & Lee, S.-H. (2017). Cografting astrocytes improves cell therapeutic outcomes in a Parkinson's disease model. *Journal of Clinical Investigation*, *128*(1), 463–482. https://doi.org/10.1172/JCI93924
76. Sorrentino, Z. A., Giasson, B. I., & Chakrabarty, P. (2019). α-Synuclein and astrocytes: tracing the pathways from homeostasis to neurodegeneration in Lewy body disease. *Acta Neuropathologica*, *138*(1), 1–21. https://doi.org/10.1007/s00401-019-01977-2
77. Spillantini, M. G., Schmidt, M. L., Lee, V. M.-Y., Trojanowski, J. Q., Jakes, R., & Goedert, M. (1997). α-Synuclein in Lewy bodies. *Nature*, *388*(6645), 839–840. https://doi.org/10.1038/42166
78. Steger, M., Tonelli, F., Ito, G., Davies, P., Trost, M., Vetter, M., Wachter, S., Lorentzen, E., Duddy, G., Wilson, S., Baptista, M. A., Fiske, B. K., Fell, M. J., Morrow, J. A., Reith, A. D., Alessi, D. R., & Mann, M. (2016). Phosphoproteomics reveals that Parkinson's disease kinase LRRK2 regulates a subset of Rab GTPases. *ELife*, *5*. https://doi.org/10.7554/eLife.12813
79. Streubel-Gallasch, L., Giusti, V., Sandre, M., Tessari, I., Plotegher, N., Giusto, E., Masato, A., Iovino, L., Battisti, I., Arrigoni, G., Shimshek, D., Greggio, E., Tremblay, M.-E., Bubacco, L., Erlandsson, A., & Civiero, L. (2021). Parkinson's Disease–Associated LRRK2 Interferes with Astrocyte-Mediated Alpha-Synuclein Clearance. *Molecular Neurobiology*, *58*(7), 3119–3140. https://doi.org/10.1007/s12035-021-02327-8
80. Stykel, M. G., Humphries, K. M., Kamski-Hennekam, E., Buchner-Duby, B., Porte-Trachsel, N., Ryan, T., Coackley, C. L., Bamm, V. V., Harauz, G., & Ryan, S. D. (2021). α-Synuclein mutation impairs processing of endomembrane compartments and promotes exocytosis and seeding of α-synuclein pathology. *Cell Reports*, *35*(6), 109099. https://doi.org/10.1016/j.celrep.2021.109099
81. Tsunemi, T., Ishiguro, Y., Yoroisaka, A., Valdez, C., Miyamoto, K., Ishikawa, K., Saiki, S., Akamatsu, W., Hattori, N., & Krainc, D. (2020). Astrocytes Protect Human Dopaminergic Neurons from α-Synuclein Accumulation and Propagation. *The Journal of Neuroscience*, *40*(45), 8618–8628. https://doi.org/10.1523/JNEUROSCI.0954-20.2020
82. Victoria, G. S., & Zurzolo, C. (2017). The spread of prion-like proteins by lysosomes and tunneling nanotubes: Implications for neurodegenerative diseases. *Journal of Cell Biology*, *216*(9), 2633–2644. https://doi.org/10.1083/jcb.201701047
83. Wakabayashi, K., Hayashi, S., Yoshimoto, M., Kudo, H., & Takahashi, H. (2000). NACP/α-synuclein-positive filamentous inclusions in astrocytes and oligodendrocytes of Parkinson's disease brains. *Acta Neuropathologica*, *99*(1), 14–20. https://doi.org/10.1007/PL00007400
84. Wang, L., Wu, D., Robinson, C. V., Wu, H., & Fu, T.-M. (2020). Structures of a Complete Human V-ATPase Reveal Mechanisms of Its Assembly. *Molecular Cell*, *80*(3), 501-511.e3. https://doi.org/10.1016/j.molcel.2020.09.029

85. Wang, X., Bondar, V. V, Davis, O. B., Maloney, M. T., Agam, M., Chin, M. Y., Cheuk-Nga Ho, A., Ghosh, R., Leto, D. E., Joy, D., Calvert, M. E., Lewcock, J. W., Di Paolo, G., Thorne, R. G., Sweeney, Z. K., & Henry, A. G. (2023). Rab12 is a regulator of LRRK2 and its activation by damaged lysosomes. *ELife*, *12*. https://doi.org/10.7554/eLife.87255
86. Wong, Y. C., & Krainc, D. (2017). α-synuclein toxicity in neurodegeneration: mechanism and therapeutic strategies. *Nature Medicine*, *23*(2), 1–13. https://doi.org/10.1038/nm.4269
87. Yang, Y., Song, J.-J., Choi, Y. R., Kim, S., Seok, M.-J., Wulansari, N., Darsono, W. H. W., Kwon, O.-C., Chang, M.-Y., Park, S. M., & Lee, S.-H. (2022). Therapeutic functions of astrocytes to treat α-synuclein pathology in Parkinson's disease. *Proceedings of the National Academy of Sciences*, *119*(29). https://doi.org/10.1073/pnas.2110746119
88. Zhou, C., Huang, M., Wang, S., Chu, S., Zhang, Z., & Chen, N. (2024). Tunneling nanotubes: The transport highway for astrocyte-neuron communication in the central nervous system. *Brain Research Bulletin*, *209*, 110921. https://doi.org/10.1016/j.brainresbull.2024.110921
89. Zuchero, J. B., & Barres, B. A. (2015). Glia in mammalian development and disease. *Development*, *142*(22), 3805–3809. https://doi.org/10.1242/dev.129304
90. Zurzolo, C. (2021). Tunneling nanotubes: Reshaping connectivity. *Current Opinion in Cell Biology*, *71*, 139–147. https://doi.org/10.1016/j.ceb.2021.03.003
91. Zygogianni, O., Antoniou, N., Kalomoiri, M., Kouroupi, G., Taoufik, E., & Matsas, R. (2019). In Vivo Phenotyping of Familial Parkinson's Disease with Human Induced Pluripotent Stem Cells: A Proof-of-Concept Study. *Neurochemical Research*, *44*(6), 1475–1493. https://doi.org/10.1007/s11064-019-02781-w